

# Lawrence Berkeley National Laboratory

## Recent Work

### **Title**

Chapter IV.2. Polymeric electrolytes: An overview

### **Permalink**

<https://escholarship.org/uc/item/8h40547p>

### **Author**

Kerr, John B.

### **Publication Date**

2003

## Chapter IV. 2.

### Polymeric Electrolytes: an overview

**John B. Kerr**

*Lawrence Berkeley National Laboratory,  
Berkeley, California, 94720, USA*

#### **Introduction.**

Ionically conducting polymers have been the focus of much fundamental and applied research for many years. Polyelectrolyte membranes have found significant technological use in the production of chlorine and caustic soda<sup>1</sup>, as separators in fuel cells<sup>2, 3</sup> and in electro dialysis<sup>4, 5</sup> for example. The discovery of ionic conductivity in polyethylene oxide solutions of alkali metal salts<sup>6, 7</sup> led the way for the introduction of polymer electrolyte in devices such as lithium batteries and electrochromic windows<sup>8, 9</sup>. Since those early days many books<sup>10-13</sup>, book chapters<sup>8</sup> and reviews<sup>9, 14-19</sup> have been published on these materials and the reader is referred to these for more detailed information.

In a recent article Scrosati and Vincent<sup>15</sup> have listed the desired properties of a polymer electrolyte for use in lithium batteries. These are adequate conductivity, high cation mobility, good mechanical properties, good interfacial contact with electrodes, wide electrochemical stability, chemical and thermal stability, safety and ease of processing. This set of properties is understandably difficult to obtain in a single material and a number of different classes of polymer electrolyte materials have been defined which possess most but not all of the desired properties. Wright<sup>14</sup> has further elaborated on this classification and defined them as:

1. Solvent-containing gel and hybrid systems.
2. Solvent-free, ion-coupled systems.
3. "Single-ion" systems and systems with reduced anion mobility.
4. Decoupled systems.

These classifications are useful for distinguishing different mechanisms of ion transport in the bulk separator. However, the complete property requirements are most easily appreciated in the context of the lithium battery application and it is a purpose of this

chapter to attempt to link the theoretical considerations of ion transport with the practical requirements of the battery in order to provide a rationale for material selection. For this we shall explore a mix of quantum chemistry, molecular dynamics, synthesis, mechanical and transport property measurements with system modeling and chemical reactivity considerations. Although this is by no means an exhaustive survey of useful techniques and approaches, it is hoped that it will provide an overview of the methods available to study the problems involved in preparation and use of polymer electrolytes.

### Lithium ion transport in lithium batteries.

Rigorous performance demands are made by battery engineers on organic electrolyte solutions in rechargeable lithium batteries. These materials, whether liquids, gels or polymers, are in intimate contact with strongly reducing lithium metal or lithiated carbon and with reactive, highly oxidizing metal oxides related to materials widely used for catalysis in other fields of technology. Figure 1 shows a schematic diagram of a typical lithium battery system which shows the basic components and the role of the electrolyte in separating the electrodes while facilitating the passage of lithium ions between them.

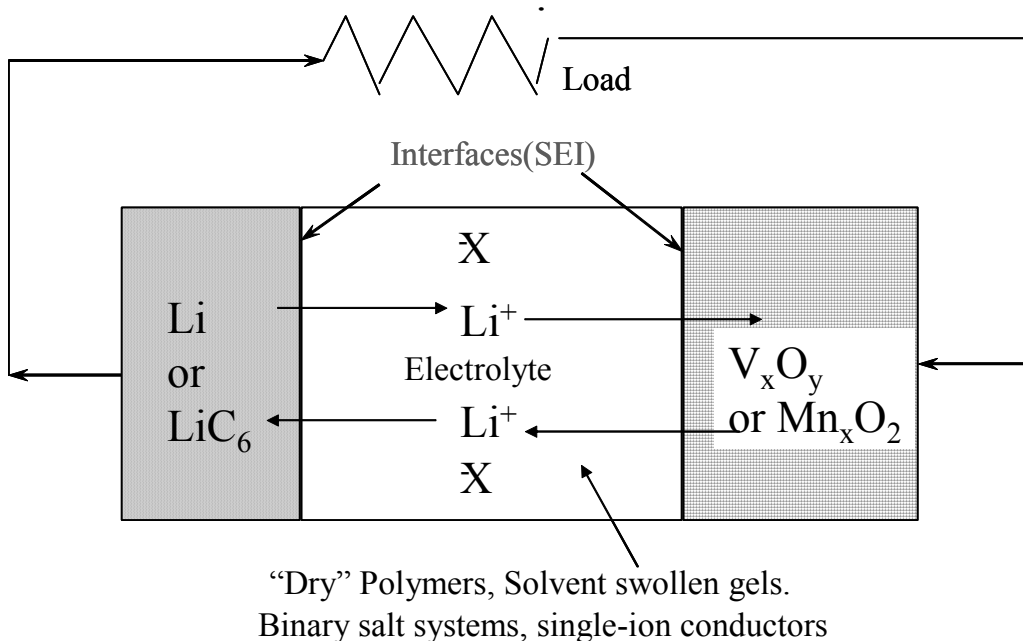


*Figure 1.* Schematic diagram of a rechargeable lithium battery (relative thickness of the electrolyte exaggerated relative to the electrodes).

In any rechargeable lithium battery capable of achieving desirable performance three main processes must occur. Lithium ions must pass from the anode into the solution, ions must be transported across the separator efficiently (good lithium ion transport properties) and react or be intercalated efficiently and reversibly at the cathode. Since the battery should be recharged, the process must be reversed with very high efficiency (>99.99%) in order to achieve a high cycle life. In addition the electrolyte must not react with the electrodes while the battery is at open circuit thereby providing a long

calendar life (15 years for electric vehicle use). Since no organic compound is thermodynamically stable to 0 volts vs. lithium metal, these requirements are stiff indeed! Fortunately, the formation of surface films at the electrodes limits the extent of these reactions and reduces the rates to levels that allow the useful cycle and calendar life of the battery to be achieved. An extensive review on this topic has recently appeared<sup>20</sup> to which the reader is referred. For the present discussion however, it is important to note that these surface films provide layers with very different transport properties from the bulk electrolyte and through which the lithium ions must pass. These layers are frequently referred to as the solid electrolyte interphase or SEI and they play a crucial role in both the cycle life and also in the rate capability of the battery.

Although chemical and thermal stability of the bulk electrolyte would seem to be a prerequisite for long life, the most commonly used liquid electrolytes in Li-ion batteries (ethylene carbonate/dimethyl carbonate/LiPF<sub>6</sub>) are not stable on standing<sup>21</sup>. They have been shown to react on standing to form transesterification products, a reaction that is catalyzed by the presence of acids or bases in the electrolytes. Such acids and bases can be formed through oxidation or reduction reactions at the electrodes or they may be present in the electrolyte itself either as an impurity (HF) or an intrinsic property of one of the components. LiPF<sub>6</sub>, LiBF<sub>4</sub> and LiAsF<sub>6</sub> have all been shown to generate the Lewis acids PF<sub>5</sub>, BF<sub>3</sub> and AsF<sub>5</sub> which are known to catalyze the ring-opening polymerization of ethylene carbonate<sup>22</sup> to polyethylene ether carbonates and other polymer materials with the accompanying production of CO<sub>2</sub> gas. Even though these electrolytes appear to be unacceptably reactive, the reactions play an important role in the formation of the SEI and hence the cycle and calendar life of the battery.

Prior to the development of intercalation anodes for lithium ion batteries, much attention was given to the behavior of the rechargeable lithium metal electrode with liquid electrolytes such as 1,3-dioxolane<sup>23-25</sup>, THF and 2-methyltetrahydrofuran (2-MeTHF)<sup>25-27</sup> containing LiClO<sub>4</sub>, LiBR<sub>4</sub> and LiAsF<sub>6</sub> salts. The Lewis acidity of the AsF<sub>5</sub> formed from the AsF<sub>6</sub><sup>-</sup> was found to play a crucial role in forming surface layers that enhance the cycling efficiency. Impressive cycle lifetimes were obtained for the lithium electrode under certain conditions (L<sub>I</sub>FOM > 100). Parameters such as the purity of the electrolyte and the lithium metal, prior history (exposure to heat or light), presence of surface-active additives or impurities and cell stack pressure were all found to affect the results. With lithium metal electrodes, loss of capacity was found to be due to chemical reactions and morphological changes that convert the lithium into a form that is not easily recoverable. This can be insoluble lithium salts or isolation of lithium metal through dendrite growth that produces “mossy” lithium. The suppression of lithium dendrite growth was and still remains a critical safety and reliability issue that could not be easily solved with liquid electrolytes. The reaction of volatile and flammable organic solvents with finely divided lithium powder was found to be an insurmountable safety problem. Polymer electrolytes, however, are not volatile and although they do react with lithium metal and oxidizing metal oxides<sup>28</sup> the slow delivery of fuel to the reaction site limits the rate of reaction and prevents runaway reactions. This safety feature plus a perception that polymer electrolytes inhibit dendrite growth have led to the intense interest in solvent-free materials over the last twenty years.

## Solvent-free, ion-coupled systems.

The commonest polymer electrolyte investigated has been based on polyethylene oxide which is commercially available in a relatively pure state at reasonable cost. It was found by Wright that the polymer could dissolve alkali metal salts to provide ionic conductivity. Figure 2 illustrates how the polymer achieves the dissolution of the salts by complexation of the metal ions via binding interactions between the ether oxygens and the metal ions. As shown in Figure 2 it is possible to bind the ions via one or more chains depending on the metal ion and the structure of the polymer chain itself. The figure shows that the number of donor atoms bound to the metal ion may also vary and in a dynamic fashion that gives rise to the movement of the ions along the polymer chains. The interaction of the anion is also shown where the anion binds or is ion-paired to the cation to form a neutral or even a negatively charged cluster species. The figure shows contact ion-pairs although solvent separated ion pairs are also possible. Intuitively, it is expected that the conductivity of the material will be favored by the formation of a higher concentration of charged species. Reduction of the ion-pair binding strength may be achieved by the use of anions such as bis(trifluoromethylsulfonyl) imide ((CF<sub>3</sub>SO<sub>2</sub>)<sub>2</sub>N<sup>-</sup>), often referred to as TFSI or imide, which delocalize the negative charge over the large anion structure<sup>29</sup>. The anion in this case is dissociated from the cation and does not interact significantly with the polymer chains. Its motion requires free volume between the polymer chains.

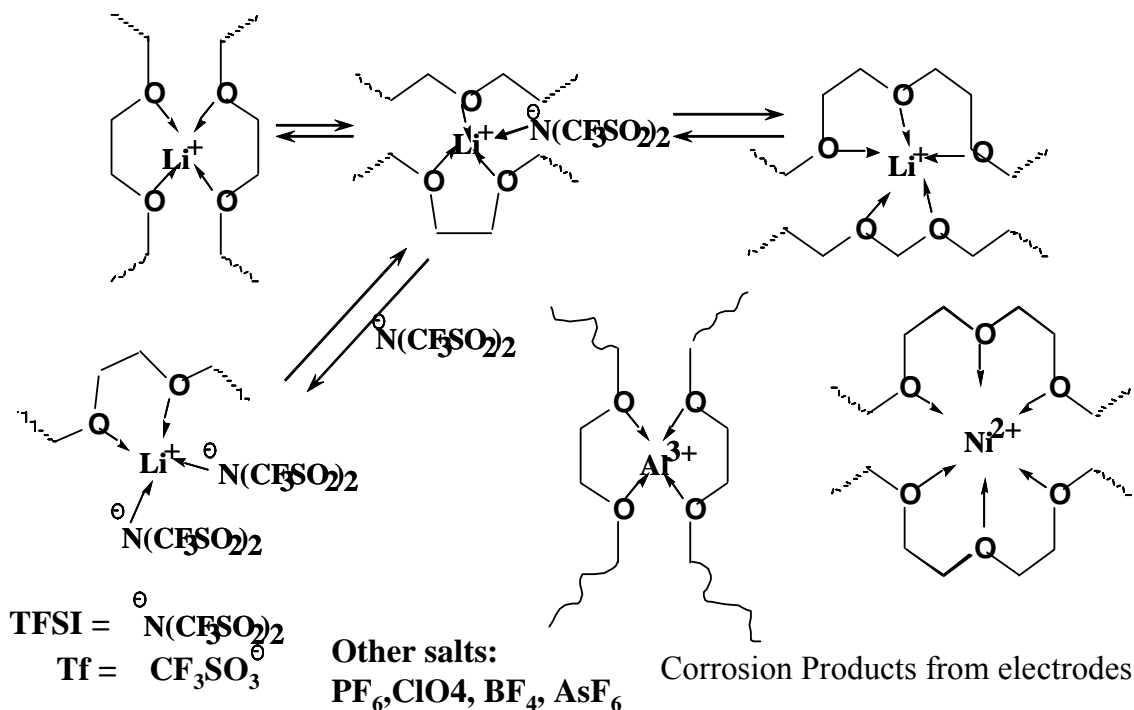


Figure 2. Solvation of Lithium and other metal ions by polyethylene oxide

In parallel with the decreased binding of the lithium ion with the anion, the strength of binding (or solvation) to the polymer increases. Thus, although there is a higher concentration of free lithium ions, they are more tightly bound to the polymer and mobility is restricted by the need to break the stronger bond in order to move along the polymer chain or from one chain to another. It was found early in the study of polymer electrolyte salt solutions that the most significant contribution to conductivity occurred through the amorphous phase where there is segmental motion of the polymer chains. Although the crystalline phases are of significant interest in order to understand the thermodynamics and conformations of the ion-polymer complexes<sup>30, 31</sup>, the ionic conduction through these immobile phases is much slower. Thus the semi-crystalline PEO-lithium salt electrolytes exhibit reduced conductivities at temperatures below the melting point of the complex. Similarly, the conductivity falls precipitously at temperatures below the glass transition temperature ( $t_g$ ) where the segmental motion of the polymer ceases and the chains are immobilized. This evidence demonstrates the strong coupling between the polymer chain motion and the mobility of the lithium ions.

A rule of thumb for the design of a polymer electrolyte is therefore to prevent crystallization and to reduce the  $t_g$  as much as possible. The larger the difference in temperature between the operating temperature and the  $t_g$ , the more vigorous is the segmental motion. Unfortunately, both crystallinity and high  $t_g$  are linked to good mechanical properties (shear modulus, tensile strength, creep compliance), which are necessary to prepare practical materials that will act as separators as well as electrolytes. A major goal of polymer electrolyte design is to de-couple the ion transport from the mechanical properties.

Effect of Polymer Molecular Structure (Architecture).

**PEO :-**  $\text{-(CH}_2\text{CH}_2\text{-O)-}_n\text{-}$  M.Wt. >  $10^6$  \$4-8/lb

**PEMO :-** M.Wt. ~ 150k  
- Oxymethylene-linked PEG400

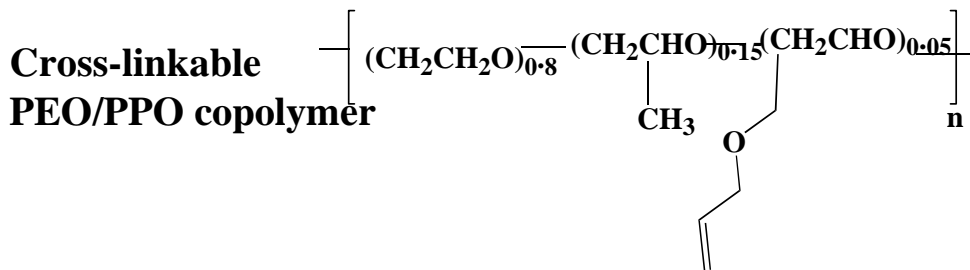
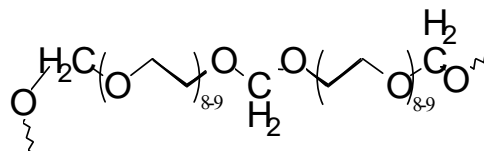


Figure 3. Linear chain polymers

A first approach is then to alter the structure of the polymer to remove the crystallinity, at least in the temperature range of interest. Figure 3 shows the chemical structures of commercial PEO, PEMO (also known as oxymethylene-linked polyethylene glycol 400 or amorphous PEO<sup>32</sup>) and a PEO/PPO/AGE co-polymer patented by HydroQuebec<sup>33</sup> (PPO = polypropylene oxide; AGE = allyl glycidyl ether). These are all linear chain polymers and the latter two polymers exhibit significantly less crystallinity and lower melting points than PEO. In fact, the polymer complexes with LiTFSI exhibit no sign of a melting transition in DSC measurements down to -100°C. The introduction of the oxymethylene link, the propylene oxide group or the allyl ether group prevent crystallization due to the irregularity of the chains that disrupts the packing of the chains into regular forms necessary for crystallization. The glass transition temperatures of these linear polymers are all less than -65°C and hence they are viscous liquids with moderate mechanical properties for high M.Wt. (> 500k) samples.

All of the polymers shown in Figure 3 may be cross-linked after film formation by reaction with radical species such as those provided by AIBN or UV radiation. However, this is quite uncontrolled chemistry that may result in a non-uniform material as the reactive radical intermediates are quite unselective. Over reaction results in a high density of cross-links, leading to an increase in  $t_g$ , reduced segmental motion and lower conductivity. Non-uniform cross-linking (or curing) yields non-uniform current densities through the membrane which will lead to rapid failure (e.g. dendrite growth). The allyl ether group, however, may be selectively reacted with hydrosilyl cross-linkers<sup>34, 35</sup> to provide uniform films from the more controlled and selective chemistry. It is worth noting that commercially available PEO contains butylated hydroxytoluene (BHT) to inhibit attack on the polyether chains by radical species formed from oxygen or light. Higher M.Wt. grades of PEO are actually prepared by radiation cleavage of very high M.Wt. PEO ( $5-8 \times 10^6$ ) which illustrates the sensitivity of these materials to radiation.

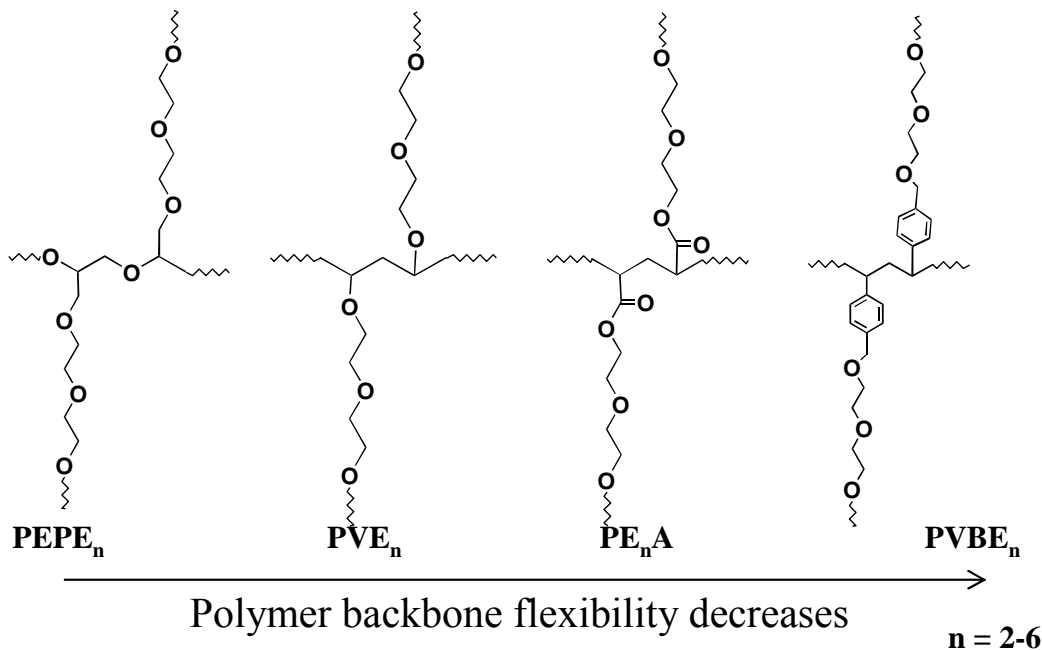


Figure 4. Comb Polymers. Optimum side Chain Length = 5-6 EO Units.

Figure 4 shows a series of comb polymers with different backbones and side chains containing ethylene oxide (EO) units similar to those in PEO. The materials are completely amorphous at all temperatures. The optimum length of the side chains is found to be between 5-6 EO units due to the appearance of crystallinity as the length of the side chains grows and resembles PEO. For shorter side chains the influence of the backbone is stronger and leads to lower conductivity. The polymer backbone influences the conductivity due to the stiffness (polystyrene) and polarizability (polyacrylate). In these cases short side chains (2-4 EO units) lead to reduced conductivity<sup>36, 37</sup>. The PEPE<sub>x</sub> and PVE<sub>x</sub> polymers show less sensitivity to the side chain length as their backbones are more flexible<sup>38-44</sup>. Polyphosphazene<sup>45-47</sup> and polysiloxane<sup>48, 49</sup> backbones exhibit similar properties as do highly branched polymer architectures<sup>50-53</sup>. The  $t_g$  values for the comb polymers are lower than for the linear polymers and their mechanical properties are much more liquid-like due to the molecular shape.

The conductivities of the polymers in Figures 3 and 4 are shown in Figure 5 as a function of temperature for polymer-salt complexes with lithium TFSI at a salt concentration of one lithium ion to 20 or 30 oxygens in the polymer. One can immediately note the lower conductivity of the PEO electrolyte at low temperatures due to the crystallinity. The linear amorphous polymer solutions show higher conductivity at low temperatures consistent with the lack of crystallinity while the comb materials show even higher conductivity at low temperature, which is consistent with greater segmental motion due to the more freely moving side chains that have free end groups<sup>51</sup>. All of the materials show the familiar convex, bent shape that has the VTF form related to the polymer chain motion. For rechargeable lithium batteries, acceptable performance for electric vehicle and typical consumer applications requires a conductivity of between  $10^{-4}$  and  $10^{-3}$  S/cm. Thus PEO performs adequately at 80°C but no system provides acceptable transport properties at ambient temperatures. In order to provide adequate performance at low temperatures it is important to elucidate the factors that control the dependence of transport properties on temperature.

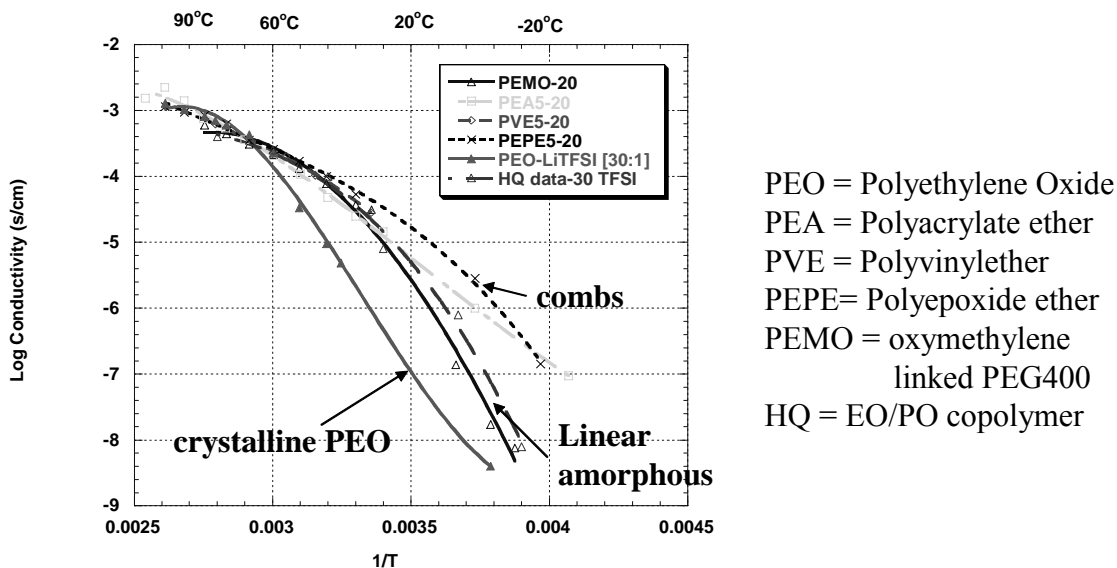


Figure 5. Comparison of conductivities of comb-branch polymer electrolytes (20:1 LiTFSI) with linear and networked co-polymers (HQ data USP #5,755,985)



### Effect of Polymer Solvation Structure.

The foregoing results provide an example of how change of the molecular structure may lead to improved ion transport through an increase of the polymer chain mobility. Much research effort has been expended in the synthesis of novel polymer structures to increase the lithium ion mobility but no true, dry polymer electrolyte has been shown to provide better performance than the comb materials shown here. The effects of the architecture change upon the conductivities are generally greatest at temperatures below 40°C. Above this temperature one may note that all the materials exhibit nearly identical conductivity dependence with temperature. This is Arrhenius dependence and is consistent with a process with an activation energy involving the making and breaking of chemical bonds. Since all of the polymers use ethylene oxide units (EO) to solvate the lithium ions it seems reasonable that the rate determining process involves breaking and forming oxygen-lithium bonds that occur in the same way for all polymers containing EO solvation units. Thus, at low temperatures close to the glass transition the segmental motion of the polymer chains is the slow process. At higher temperatures this motion increases to a point where the rearrangement of the solvation sphere becomes rate determining. This is illustrated schematically in Figure 6 which shows an exaggerated motion of a comb polymer side chain combined with the solvent rearrangement as the ion moves from one chain to the next. Recent neutron scattering experiments have provided support for this scheme<sup>54-56</sup> through the identification of two distinct types of relaxation.

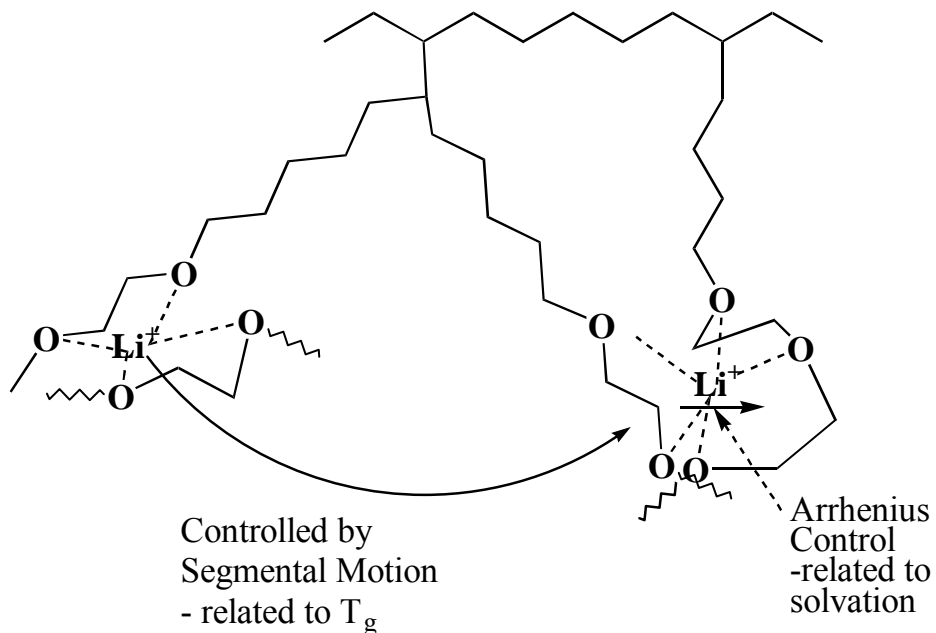


Figure 6. Schematic contributions of segmental motion and solvation to ionic mobility.

The mechanism of the solvent reorganization around the ion is of crucial importance as it controls the height of the activation barrier to movement of the bound ion and hence the slope of the temperature dependence of conductivity. In order for the

ion to move the solvated ion passes through an activated complex. This may be formed by dissociation of an oxygen-lithium bond to form a less coordinated complex followed by formation of a new  $\text{Li}^+\text{-O}$  bond to a different point in the chain or on a new chain. An alternative mechanism would involve an increase in the coordination number in the activated complex with either the same chain or a second chain (or segment). The rearrangement involving multiple chains will be slower as a result of the decreased entropy of the intermediate complex in the case of either mechanism and may imply that chain to chain transfer is rate determining.

If the nature of the solvation is rate determining for ion mobility there should be a change in the temperature dependence of the conductivity upon a change of the groups involved. Figure 7 shows a comparison of a number of polymers complexed with LiTFSI. In particular, those that contain propylene oxide units ( $\text{CH}_2\text{CH}(\text{CH}_3)\text{O}$ ), carbonate ( $\text{OCOO}$ ) and trimethylene oxide (TMO,  $\text{CH}_2\text{CH}_2\text{CH}_2\text{O}$ ) appear to show different temperature dependences at temperatures above  $40^\circ\text{C}$  where segmental motion is not rate determining. In comparison, a liquid or gel electrolyte shows less pronounced temperature dependence in this range than any of these electrolytes due to the vehicular mechanism of ion transport. For liquids and gels the solvent molecules travel with the ions so the bond breaking and forming is less important to the ion transport.

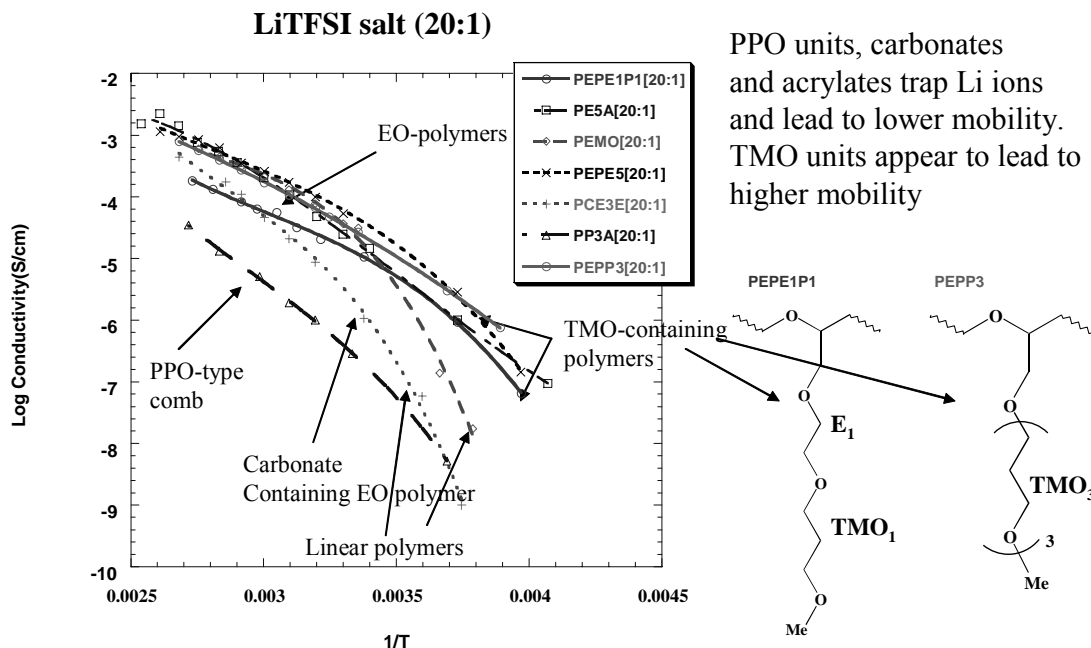
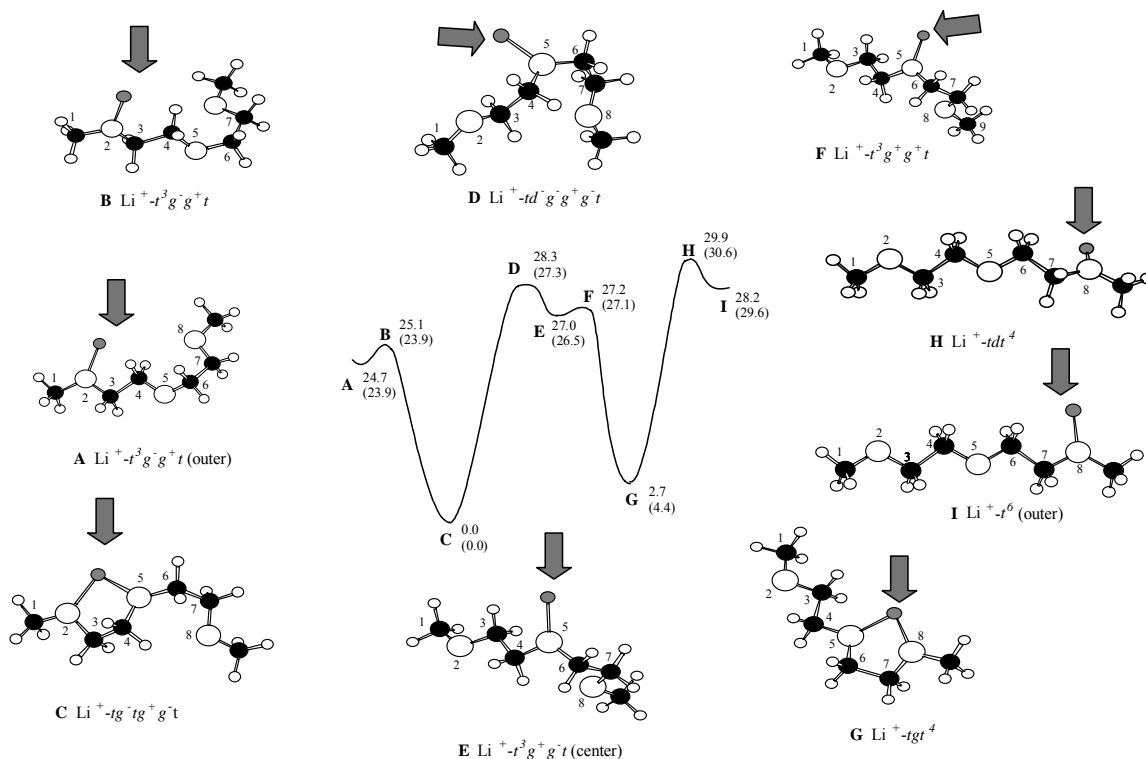


Figure 7. Temperature dependence of conductivity for polymer electrolytes containing different solvation groups.

These results indicate that there is scope to improve the ambient temperature performance of polymer electrolytes by variation of the solvating groups. However, this involves considerable synthetic effort to introduce new groups such as TMO, carbonate or new donor atoms such as nitrogen, sulfur or phosphorus. The use of molecular modeling is an invaluable aid to guide the synthesis direction since it may eliminate

unpromising structures before an extensive effort is made to prepare appropriate polymers. There is an extensive literature on different levels of modeling for polymer electrolytes<sup>10, 17, 57-62</sup>. Among this work are some calculations relevant to the polymer structures whose conductivities are shown in Figure 7. Quantum chemical calculations have been carried out to estimate the binding strength of lithium ions to polyalkyl oxides as a function of the coordination number (1-6) and the nature of the solvating group (EO, PO and TMO)<sup>63</sup>. These calculations show that the binding energy of the TMO groups are higher for TMO than for PO and EO at coordination numbers up to 6 when the steric crowding of the TMO forces a longer Li –O bond length and the binding energies drop below those of the EO and PO. This is consistent with early literature reports that polyTMO polymers did not dissolve lithium salts<sup>64</sup>. Methods of estimating the height of the activation barrier for movement of the lithium ion along the polymer chain have been developed based on a mechanism that involves an intermediate with a lower coordination number<sup>65, 66</sup> and a comparison of polymer structures containing EO and TMO groups indicates that the barriers are lower for the TMO polymers<sup>67</sup>. Figure 8 illustrates the movement of the lithium ions along the polymer chain where the arrow points to the lithium ion and illustrates the method of calculation.



**Figure 8.** Calculated reaction pathway for migration of the lithium cation along a polyethylene oxide (PEO) chain. The PEO is modeled by diglyme and the cation moves by making and breaking Li-O bonds. The energies are in kcal/mol from HF/6-31G\* calculations<sup>63, 67</sup>.

The theoretical calculations indicate that the migration of the lithium ion along the polymer chain will be faster for a TMO polymer compared to an EO polymer. Comb

polymers have been prepared with varying contents of EO and TMO units and the temperature dependence of conductivity, the glass transition temperature as a function of salt concentration are shown in Figure 9. The polymers in this case are the polyepoxide ether polymers with different proportions of EO and TMO units in the side chains which vary from all EO to all TMO units<sup>67, 68</sup>. It can be clearly seen that as the proportion of TMO in the polymer increases the low temperature conductivity increases and the dependence of  $t_g$  upon the salt concentration decreases. However, it is very striking that the temperature dependence of the conductivity above 40°C is unaffected indicating that the motion along the chain as calculated is not rate determining.

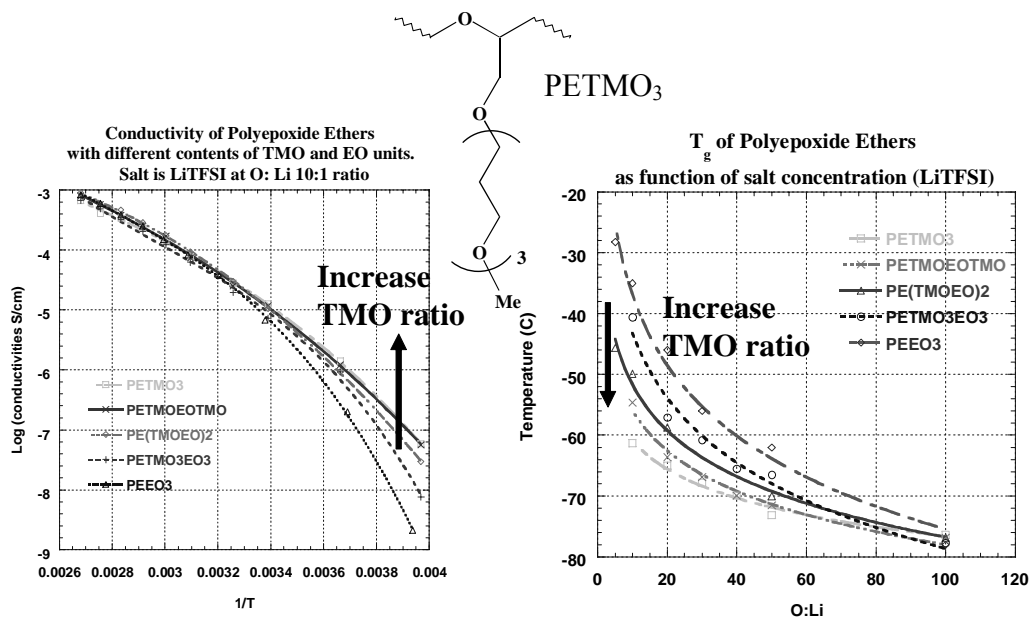


Figure 9. Conductivity as a function of temperature and glass transition temperature as a function of Li TFSI salt concentration for comb polymers with structures like the PETMO<sub>3</sub> shown but with some or all of the TMO units exchanged for EO.

There are a number of significant differences between these comb polymers (presence of PO units in the backbone, chain ends with OH groups) and the linear polymer chain used for the calculations but it appears that the mechanism used in the calculations does not dominate the rate. Measurements of the linear PTMO-LiTFSI complexes show a slightly shallower slope but no overall increase in conductivity over the linear PEO systems which indicates that the differences in the comb structure are not significant. The decreased dependence of the  $t_g$  on salt concentration observed for both comb and linear TMO polymers indicates that the ionic cross-linking between chains is reduced with TMO. Although this does not solve the problem of how to obtain high conductivity at room temperature, it is an important result as the TMO structures may be used to mitigate the effects of salt concentration gradients that occur in lithium-polymer batteries, particularly in the presence of surfaces such as electrodes or ceramic filler particles.

The results of these combined synthetic and theoretical efforts have yet to establish the physical phenomena that limit the mobility of the ions. However, the possibilities have barely been explored as there many structures such as carbonates, polyethylene imide (PEI) and polyalkylsulfide (PES)<sup>61</sup> that may be synthesized to test the limitations of these electrolyte systems. To date, the barrier to ion transport remains undefined in the simple systems. Efforts have been made to investigate the influence of different phases such as the use of block copolymers<sup>69-74</sup> that provide different environments for the solvated ions, rigid polymer systems such as glassy<sup>75</sup> or crystalline<sup>76</sup> electrolytes that contain defects as well as “polymer-in-salt” systems<sup>77</sup>. These approaches show promise to provide information that will elucidate the nature of the limiting process in the ionic motion although they do introduce further complexity into the system. The presence and effect of different phases on the behavior of the polymer electrolyte is of great interest not only for the effect on ionic mobility but also for the understanding of the interfacial behavior at electrode surfaces.

#### *Effect of surfaces on polymer electrolyte behavior.*

There has been much interest in the behavior of polymer electrolytes in combination with fillers such as nano-particulate fumed silica, alumina and other ceramic materials<sup>78-84</sup>. Most of these studies have been carried out with high M.Wt. PEO and have reported improvements in conductivity, transference number and interfacial behavior with lithium metal electrodes upon addition of the ceramic fillers. The effect of the fillers has been shown to be partly due to a suppression of the crystallinity of the PEO electrolyte but increases in conductivity have been observed at temperatures above the melting point of the polymer system which indicate some different mechanism is in play. It was noted many years ago that the method of electrolyte preparation and the presence of fillers could alter the mechanical and transport properties<sup>85, 86</sup> and the presence of solvent impurities and the thermal history of the semi-crystalline materials can lead to wide variations in the measured properties. Unfortunately, most of the studies are complicated by the fact that commercial PEO already contains about 3% fumed silica plus some residual calcium salts from the manufacturing process. The fumed silica is added as a desiccant and binds impurities such as water and other solvents to its surfaces.

The observation of increased ion transport with added nanoparticles at higher temperatures is not universal. Johansson and co-workers observed no increase upon the addition of fumed silica to LiTFSI solutions in PEO and PEMO<sup>84</sup>. Their observation is more consistent with reports in the rheology literature that would lead one to expect a decrease in ion transport properties. For example, Tsagaropoulos and Eisenberg have reported on the observation of a second glass transition at higher temperatures upon addition of fumed silica nano-particles to various polymers<sup>87, 88</sup>. They have ascribed this behavior to the inhibition of polymer segmental motion by interactions between the polymer and the particle surface which leads to the development of immobile layers. As the proportion of filler particles increases the immobile layers overlap leading to a distinct phase from the polymers in the bulk of the material and hence to the observation of a second  $t_g$  at values as much as 100°C above the first one (see Figure 10). The second  $t_g$  was observed using dynamic mechanical analysis but the behavior has been confirmed by recent neutron scattering measurements which showed the existence of two distinct

relaxation processes in the presence of the fillers<sup>89</sup>. The behavior is dependent upon the nature of the polymer-surface interaction, the polymer molecular weight and any cross-linking, be it covalent or ionic as in the case of a polymer electrolyte. It has been reported that for high M.Wt. polymers the second  $T_g$  is not observed but the  $T_g$  increases due to the restriction of the polymer chain motion by multiple particles<sup>90</sup>. As has been noted by Eisenberg these effects are not confined to solid polymer systems but also play a role in polymer gel systems and hence are likely to influence transport properties in composite electrolytes and electrodes in lithium ion and lithium-polymer gel batteries as well as solid “dry” polymer electrolytes.

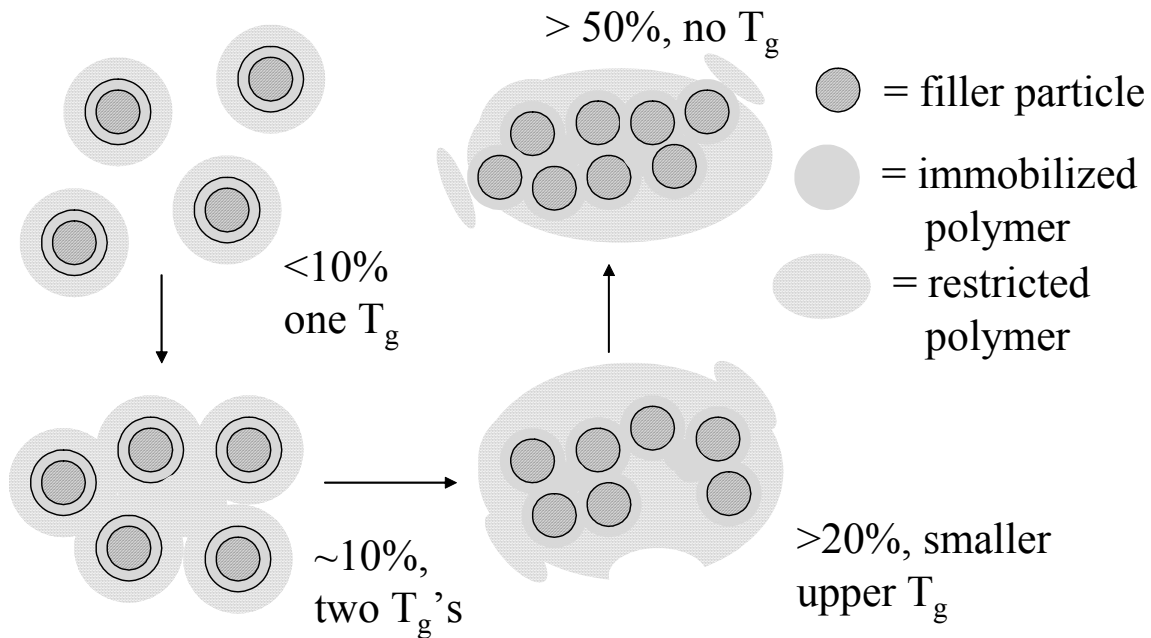


Figure 10. Eisenberg model of the effect of nanoparticles on the mobility of polymer chains.

The effect of surfaces and thin film geometries on the properties of polymers<sup>91-97</sup> is of general interest to materials scientists due to the relevance to the properties of composites, laminates and the field of adhesion<sup>98, 99</sup>. In general these effects derive from the inhibition of the polymer motion by the surface either through formation of some form of binding or by geometric restriction of some modes of motion. This accounts for the inhibition of crystallization and may in some cases result in an increase in mobility of the polymer chains close to the surface compared to the bulk. The nature of the interaction between the surface and the polymer may lead to increases of the chain motion and lower  $T_g$  values if the surface is appropriately treated to minimize the polymer-surface interaction<sup>92</sup>. On the other hand very strong polymer-surface interactions can lead to the formation of an immobile layer at the surface. If this surface happens to be an electrode it implies that the mechanism of ion transport through the surface layers at the electrode is different from the bulk polymer where segmental motion predominates. The study of nano-particle fillers may therefore be useful for understanding some of the complex processes that occur at the electrode surface in the SEI layers.

A recent study of the effects of added nanoparticles upon the ion transport and mechanical properties of PEO electrolytes has provided results that allow reconciliation of the apparently contradictory mechanical and conductivity measurements<sup>100</sup>. Firstly, PEO was purified to remove the fumed silica added by the manufacturer to provide a true measure of the PEO properties when complexed with lithium salts. This material was compared with commercial PEO containing the 3% fumed silica (lab-purified) and with commercial PEO containing added nanoparticles fillers (hydrophilic Aerosil A200 and hydrophobic Aerosil R805), 10% by weight. The conductivities are plotted against temperature in Figure 11a for the LiTFSI solutions in these PEO samples while Figure 11b shows the compression elastic modulus as a function of frequency at 80°C for the same LiTFSI-PEO samples.

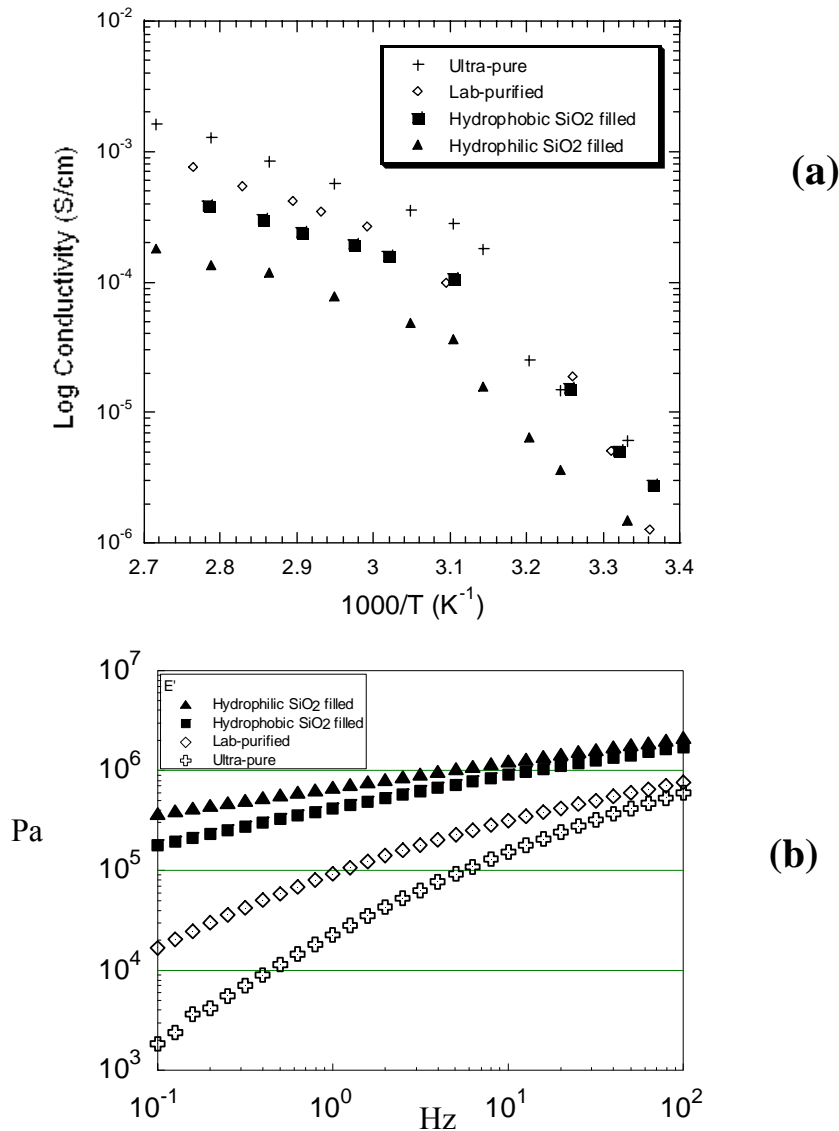


Figure 11: (a) Conductivity versus (b) compression elastic modulus (right) of low molecular weight ( $2 \times 10^5$ ) P(EO)<sub>20</sub>LiTFSI at 80°C. Amount of fumed silica added is 10%.

The results clearly show that the conductivity is higher in the absence of nanoparticles while the modulus is lower. Crystallization occurs below 60°C as seen by the break in the conductivity curve in Figure 11(a) and the presence of the filler materials does not suppress this. The compression modulus increases and the conductivity decreases as fillers are added in these experiments where care was taken to exclude moisture. A striking result, however, is that the addition of the hydrophobic filler material provides almost as much increase in mechanical strength as the hydrophilic material yet the conductivity decrease is much smaller, indicating the different effects of the surface groups. In this case the hydrophilic filler has SiOH groups on the surface while with the hydrophobic group the surface OH groups are capped with octyl groups to provide the hydrophobicity. The results illustrate the effects of the polymer–surface interaction upon the segmental motion and in this case the ionic motion appears to largely avoid the hydrophobic surface layers. It might be noted that similar interfacial effects might be expected with diblock copolymers that promote microphase separation and generate a polar/non-polar interface<sup>70, 72-74, 101</sup>.

Addition of impurities such as water through exposure of the samples to atmosphere has been shown to have an effect on conductivity for certain salt systems. In the case of the LiTFSI-PEO system exposure of the membranes to atmosphere did not result in appreciable changes in the conductivity in the presence or absence of ceramic fillers. However, for lithium triflate and lithium perchlorate systems such exposure led to an increase in the conductivity particularly in the presence of the ceramic fillers. The effect appears to be greater at low temperatures where crystallization is inhibited although increase of conductivity was observed above the melting point. Clearly, adventitious water is absorbed by the filler material to create a layer on the surface of the particles that can provide a pathway for the ions to move more easily than through the bulk of the polymer. Addition of filler particles such as activated alumina has long been used to scavenge residual water in organic solvents and electrolytes<sup>102, 103</sup> and this desiccant effect is likely the source of the reported improvements in interfacial behavior with lithium electrodes. The concentration of the water and other polar impurities on the filler surfaces provides a physical basis for the proposal of Kumar that there is a change in dipoles at the interface<sup>83</sup> and is consistent with some of the other observations concerning Lewis acidity of the surfaces<sup>78, 104</sup>.

These composite and multiphase systems are intrinsically interesting for the insight they provide into ion transport mechanisms in solid polymer electrolytes. Studies on this behavior also provide valuable information on how the electrolytes behave next to electrode surfaces and how the composite electrode structures should be formulated to obtain the best mass transport conditions in the electrolyte in confined spaces. Since similar interfacial issues arise with gels and liquids the issues raised here for the solid polymer systems are relevant for gel polymer and liquid lithium ion systems as well as fuel cell electrodes where the desired power densities and rates are very much higher.

### **Gel Polymer Systems.**

The introduction of small molecule additives or plasticizers into a solid polymer electrolyte system leads us into the area of polymer gel electrolytes. These are electrolyte systems that consist of a polymer matrix combined with a solvent system. The



salt may be dissolved in the solvent or may be attached to the polymer framework as is the case in the familiar polyelectrolyte membrane, Nafion<sup>®</sup>, used in chlor-alkali electrolyzers and in fuel cells. Two articles have recently appeared that describe polymer gel systems<sup>105, 106</sup> of the former type where polymer matrices selected from PVDF, PAN and PEO are used to form a gel with liquid electrolyte systems that are commonly used in lithium ion systems. Two types of polymer gel battery systems are generally under investigation. One is where a polymer gel is sandwiched between lithium ion battery electrodes where a different polymer (PVDF) from the separator is used as binder in the electrode<sup>107, 108</sup>. The second type is often referred to as the Bellcore system and refers to a porous polymer gel system prepared from copolymers of vinylidene fluoride with hexafluoropropylene, PVDF-HFP, and typical lithium ion battery electrolytes, LiPF<sub>6</sub>/EC-DMC<sup>109-113</sup>. In this case the polymer binder in the electrodes is identical to the polymer in the separator and the co-polymer formulation is chosen to reduce the crystallinity and optimize the uptake of solvent into the separator and electrodes. These gels often contain fumed silica particles to provide improved mechanical properties<sup>114-116</sup>. In fact, gel electrolytes with excellent mechanical properties and liquid-like transport properties have been prepared with only the presence of fumed silica particles which form a network structure that contains a polyethylene glycol dimethylether (PEGDME) solution of LiTFSI salts<sup>117-120</sup>. These systems show great promise as they combine excellent mechanical properties with high rate capability and the potential for good chemical and electrochemical stability with the electrodes while providing enhanced safety, lower cost and more flexibility in packaging than a conventional lithium ion cell.

The operation of the gel polymers is dependent upon the presence of the solvent molecules that travel with the ions just as occurs in a liquid. Thus, the conductivity and salt diffusion coefficients approach those of liquid electrolytes ( $> 10^{-3}$ S/cm,  $10^{-7}$ cm<sup>2</sup>/s at room temperature)<sup>111, 121, 122</sup>. The polymers and ceramic networks provide the mechanical strength by forming networks through which the liquid is able to migrate. This network formation is a function of the properties of the polymer or particle surface and how it interacts with the solvent cluster as it moves through the matrix. The best known system for this is the presence of clusters and multiplets that form lamellar pathways in polyelectrolyte gels as is well known for Nafion<sup>®</sup> and other polyelectrolyte membranes<sup>3, 123</sup>. As such these solvent-network interactions and gel-electrode interactions are simply extensions of the issues considered above for the effect of surfaces on dry polymers and consequently many of the considerations are similar. The ability of the network system to completely contain the liquid and prevent leakage is of great importance as is the potential for the gel to retard reactions, prevent thermal runaway and enhance safety. From a manufacturing point of view polymer gel systems are of interest as the gel precursors can be introduced into the cell as a liquid and gelled in place, thereby greatly simplifying the manufacturing process. There are, however, a number of drawbacks with this procedure that will be more apparent after discussion of the design needs of practical lithium batteries in the next section.

### **Polymer Electrolytes in Lithium Batteries.**

Since the intense interest in polymer electrolytes is nearly always justified by the use of these materials as separators in lithium batteries, it is clearly important to bear in

mind the requirements of this application. Our schematic of a lithium battery in Figure 1 may be elaborated upon as shown in Figure 12 to provide us with more insight into the conditions that the polymer electrolyte is expected to operate under. Inspection of the figure shows a lithium metal anode in contact with a polymer electrolyte where the polymer chains are represented by the thin lines and the salt ions are dispersed through the electrolyte. The lithium metal thickness and the electrolyte separator are each on the order of 30-50 $\mu\text{m}$  thick. The composite cathode is represented by the mixture of large cathode particles (vanadium, manganese or cobalt oxides) which are about 1-10 $\mu\text{m}$  in diameter, carbon black nanoparticles (10-100nm diameter), polymer chains and salt ions in a layer that is about 50-100 $\mu\text{m}$  thick. The purpose of the carbon nanoparticles is to provide an electronic conduction path from the current collector to the cathode particles. The polymer electrolyte has to function as a binder for the cathode particles so that they remain in electronic contact as well as to provide a pathway for ionic conduction through the electrode to the surfaces of the cathode particles. In the case of a gel polymer the ions with their accompanying solvent molecules must travel through the confined spaces between the electrode particles while for a dry polymer system, the polymer segmental motion must be maintained in the restricted spaces to provide ionic mobility or some other mechanism of ionic transport may operate.

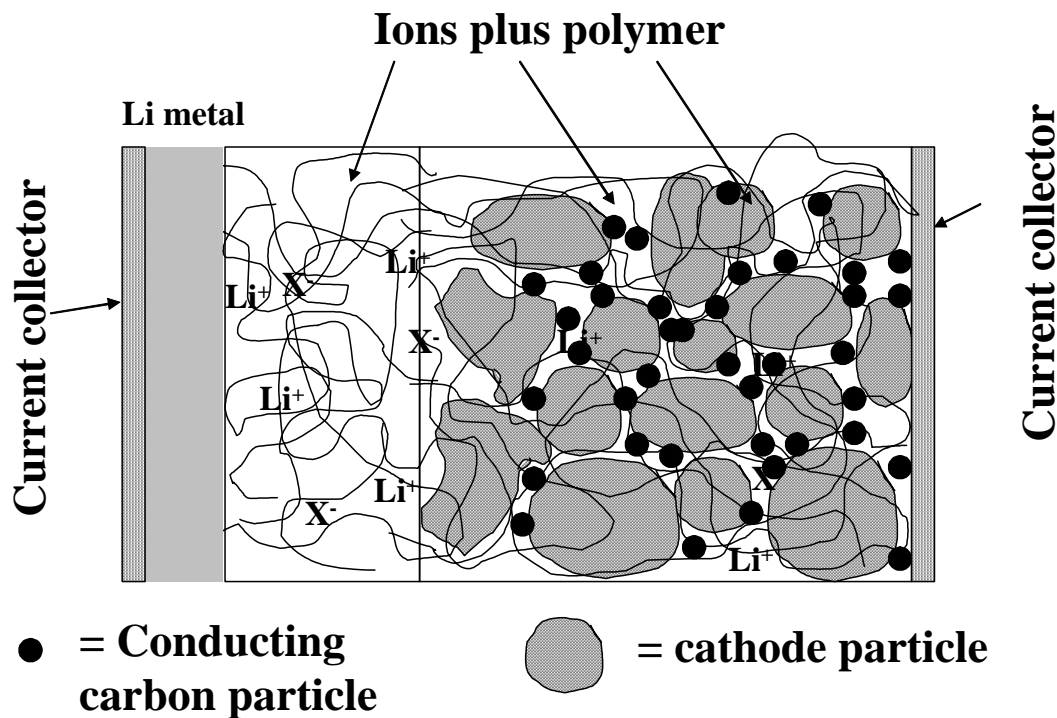


Figure 12. Schematic of a lithium polymer-metal oxide battery showing the environment for the operation of the polymer electrolyte.

Consideration of these requirements immediately provides some perspectives on the approaches that have been used to improve the conductivity of polymer electrolytes. The barriers to ionic transport occur more in the composite electrodes than in the separator<sup>110, 111, 124, 125</sup>. Hence, one can immediately see the difficulties for the

introduction into a composite electrode of glassy polymers<sup>75</sup>, composite systems with more particles<sup>78, 82, 83, 115</sup> or regular structures such as layered<sup>72-74</sup> or crystalline<sup>30, 76</sup> phases. It would be unreasonable to expect similar behavior in the composite electrode as is observed in the bulk separator. As we have seen from our discussion of the effects of surfaces on polymer dynamics, this is equally true for polymer electrolytes that depend on segmental motion or vehicular motion of solvent. While battery engineers continue to use composite electrodes this will be a challenge. However, Sadoway and Mayes have pointed out the possibilities of thin-film battery systems<sup>126</sup> and these novel systems may become more practical as large-area, thin-film technology is developed for applications such as organic and polymer light emitting diodes for area lighting for example<sup>127</sup>. In either composite or thin-film electrode systems the electrolyte will continue to have an interfacial region and therefore the study of composite polymer electrolytes will continue to provide invaluable information.

In addition to the physical changes that the electrode surfaces may impose upon the electrolytes one must also consider chemical changes that occur due to interactions between the electrodes and the electrolytes. In the case of lithium metal one can expect cleavage of carbon-oxygen bonds to occur leading to lithium alkoxides and alkyl-lithium compounds on the electrode surfaces<sup>20, 26, 128</sup>. If these lithium compounds remain connected to polymer chains the resulting strong interaction will lead to immobilization of the polymer chain close to the surface. The complex surface reactions are critical for the formation of effective SEI layers at both lithium metal, carbon and alloy electrodes<sup>20</sup> and indeed there is evidence that the salt anions may be more reactive than the polymers under some circumstances<sup>129</sup>. Corresponding oxidation chemistry is expected to occur at the cathode surfaces. Ethers are known to be oxidized at potentials less than 4V vs. Li<sup>130-132</sup> and, while carbonate solvents appear to be electrochemically stable to greater than 5V<sup>133</sup>, preceding chemical reactions may occur to yield more easily oxidized species<sup>21, 134</sup>. In any event, side reactions that involve oxidation of electrolyte at the cathode will likely generate hydrogen ions that may initiate further reactions in the organic medium which can lead to further bond formation or cross-linking. These reactions can drastically change the nature of the electrolyte-surface interaction and as we have seen this can have significant effects on polymer dynamics close to the electrodes.

The surface effects combine with the mechanical and transport properties of the bulk polymer electrolyte to provide a complicated system that is best approached from a system model point of view<sup>125</sup>. Consideration of how the system behaves in the application can be related back to the molecular models of transport and reactivity to help guide the selection and design of the appropriate materials that can provide the desired improved performance<sup>68</sup>.

### *The Effect of Transport Properties on Cell Performance.*

In the previous discussion on lithium ion mobility, the conductivity was primarily used as a measure of the effects of the various structural changes. To properly describe the transport properties of an electrolyte containing  $n$  components requires knowledge of  $(n/2)(n-1)$  transport properties. For a binary salt polymer electrolyte system these properties are conductivity ( $\sigma$ ), salt diffusion coefficient ( $D_s$ ) and transference number ( $t_+$ ) where the transference number is defined as the number of moles of ion constituent

crossing a reference plane fixed with respect to the solvent when one Faraday of current is passed<sup>135</sup>. For a gel electrolyte six transport properties would be required while for a polyelectrolyte only one is required, the conductivity. The impact of the transport properties results from the electrode processes in the cell. In most lithium ion battery systems only the lithium ion undergoes any reaction at the electrode while the anion does not undergo a reaction. Thus, when the lithium ion is removed from solution by intercalation into or deposition on to the electrode, the anion will move towards the other electrode and tend to accumulate there. This will set up a concentration gradient next to the electrode which will be relaxed by diffusion. A system with a large salt diffusion coefficient such as a liquid electrolyte will be able to relax the concentration gradient sufficiently to prevent concentration polarization from becoming a problem. The higher the current density or power requirement, the larger this needs to be in order to prevent voltage losses due to concentration polarization. The development of the concentration gradients in the lithium-polymer battery is shown schematically in Figure 13.

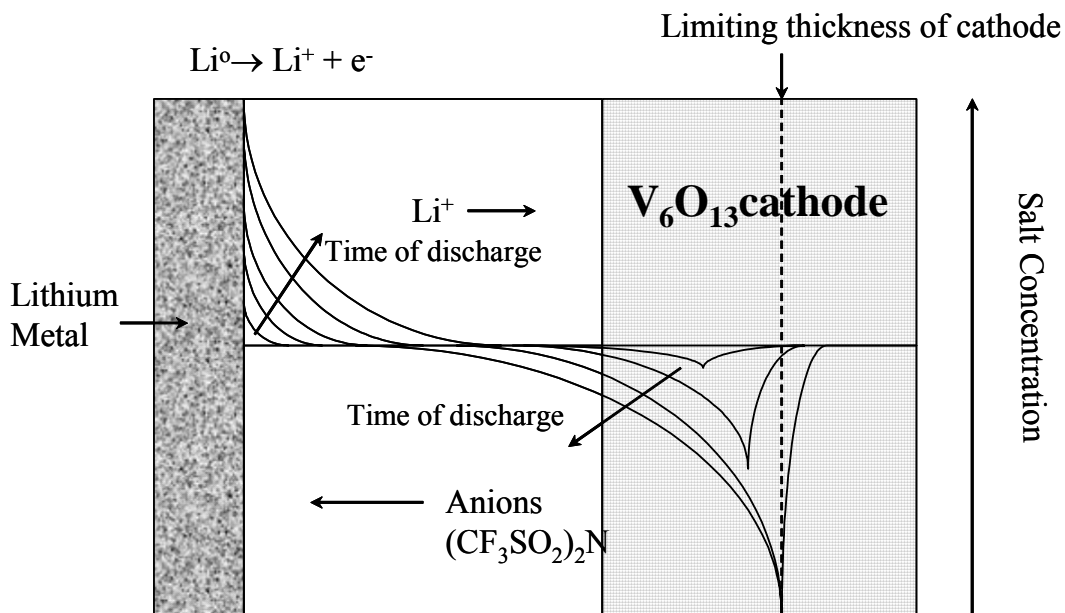


Figure 13. Effects of transference number and salt diffusion coefficient on salt concentration profiles upon Li-polymer cell discharge.

The figure shows the development of an increase in salt concentration at the anode with time of discharge while within the cathode there is a depletion of salt concentration until it reaches zero. This limits the accessibility of the cathode towards the back of the electrode. These processes are complex and have been exhaustively analyzed by the Newman group<sup>125, 136-141</sup> and the reader is referred to this body of work for detailed information. On recharging the battery the salt concentration is depleted next to the lithium electrode while the concentration increases occurs within the composite electrode. The only way to avoid these concentration gradients is to immobilize the anion on the polymer to form a polyelectrolyte where  $t_+^0=1$ . The system modeling uses concentrated electrolyte theory and porous electrode theory<sup>135</sup> to predict the behavior of

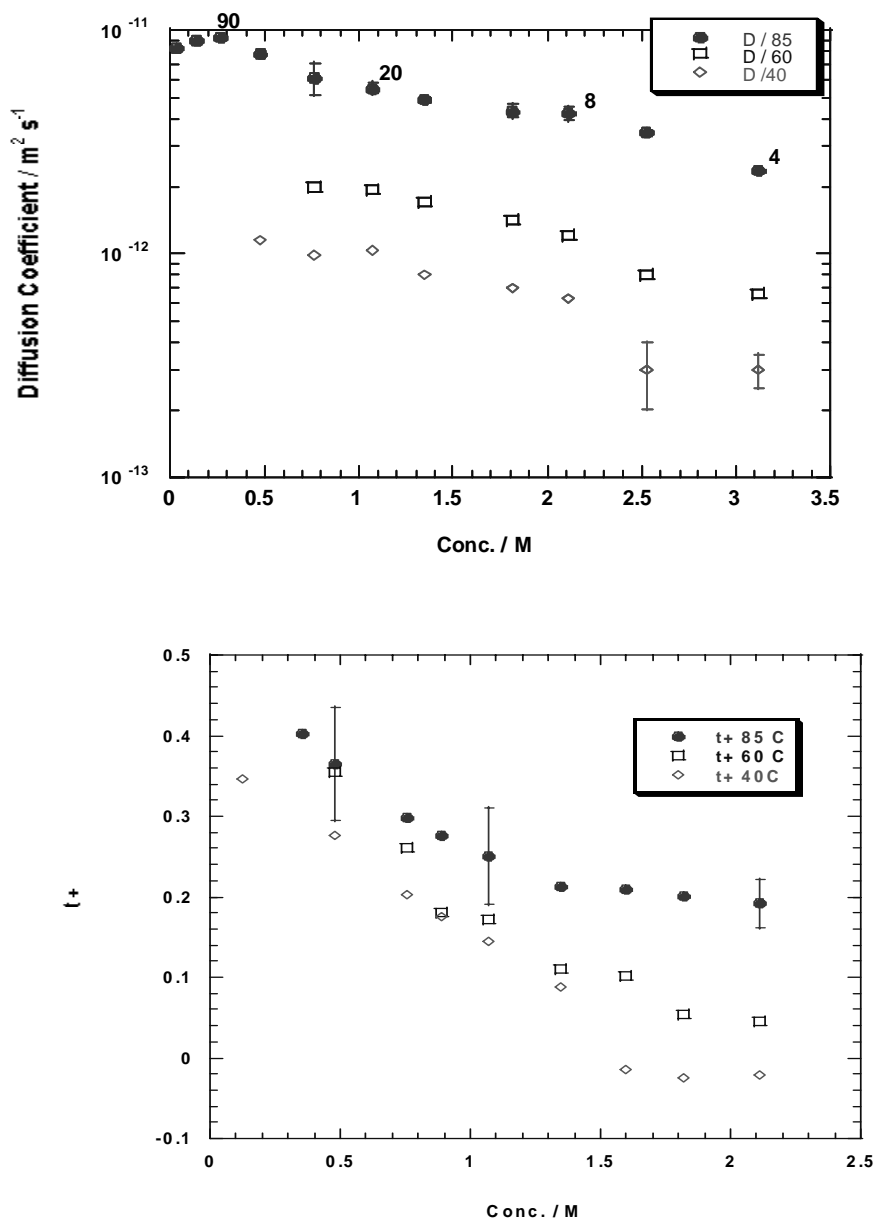


Figure 14. Salt Diffusion Coefficient ( $D_s$ ) and transference number ( $t_+$ ) for LiTFSI-PEMO as a function of salt concentration and temperature (40, 60 and 85°C).

the batteries and to successfully accomplish this requires knowledge of the transport properties in the bulk of the separator and also within the composite electrodes. Rigorous methods for measurement of transport properties in the bulk of the polymer electrolyte separator have been developed<sup>121, 122, 142-144</sup> and these have been used to provide values for a number of important systems<sup>142, 145-148</sup>. The values of the transference numbers and salt diffusion coefficients are found to vary with salt concentration and temperature for any particular system and the values for the PEMO-LiTFSI system are shown in Figure 15. It has been found that the values are affected by phase changes in the electrolyte at high concentrations and by side reactions with the lithium metal electrodes at low concentrations. However, the values in the concentration range 0.5-2.5M appear to be quite usable as they accurately predict cell behavior (e.g. limiting current at various temperatures). These numbers were used to model the lithium/polymer/V<sub>6</sub>O<sub>13</sub> system<sup>124, 125</sup> and to predict the energy and power density of the system. The analysis demonstrated that the transport properties of the PEMO-LiTFSI system at 85°C were adequate to obtain the energy and power density that is desired for electric vehicle use but that performance at lower temperatures was seriously inadequate. It is from analyses such as these that the conductivity goal of polymer electrolytes of 10<sup>-3</sup>S/cm at room temperature has evolved but it is necessary to measure all the relevant transport properties to correctly predict battery performance.

From the earlier discussion on the effects of surfaces and nano-particles on the polymer dynamics, it is not unreasonable to expect that the transport properties of the polymer electrolyte may be altered within the composite electrodes and that this may lead to performance that is different from the model predictions, particularly at high rates where the diffusional relaxation may be significantly altered by the presence of nano-particles. Some hint of this phenomenon has been noted in the comparison of the performance of Bellcore gel polymer batteries with model predictions<sup>111</sup>. Reduction of the salt diffusion coefficient by a factor of two or more was necessary in order to fit the model predictions to the high rate behavior. A similar comparison of model predictions with discharge and charge behavior has not yet been completed for lithium-polymer systems. However, examination of the cell cycling behavior by current interruption techniques indicates that the mass transport effects are very significant. Figure 15 shows the voltage profiles of discharging and charging of a lithium metal/PEO-LiTFSI/V<sub>6</sub>O<sub>13</sub> while the current is interrupted for one hour after ten minutes of current flow at 0.1mA/cm<sup>2</sup>. The insets in the figure show the relaxation of the cell at the top of charge and at the bottom of discharge. One can observe significantly larger concentration polarizations at the top of charge which is consistent with the increase of salt concentration within the cathode structure that is relaxed more slowly due to the change in transport properties within the composite. The discharge capacity declines rapidly under these cycling conditions. The correlation of capacity fading with poor transport properties has also been demonstrated for a number of electrolytes with manganese oxide cells<sup>149</sup> and the formulation of the composite electrode system has to take into account the potential effects of surface-polymer interactions on the polymer dynamics. It has been noted that modification of the carbon particle surfaces with PEG chains leads to improved cycle life<sup>150</sup> and it is common practice to include surfactants in the cathode mix that improve the cycle behavior<sup>149</sup> presumably by modifying the carbon-polymer interaction.

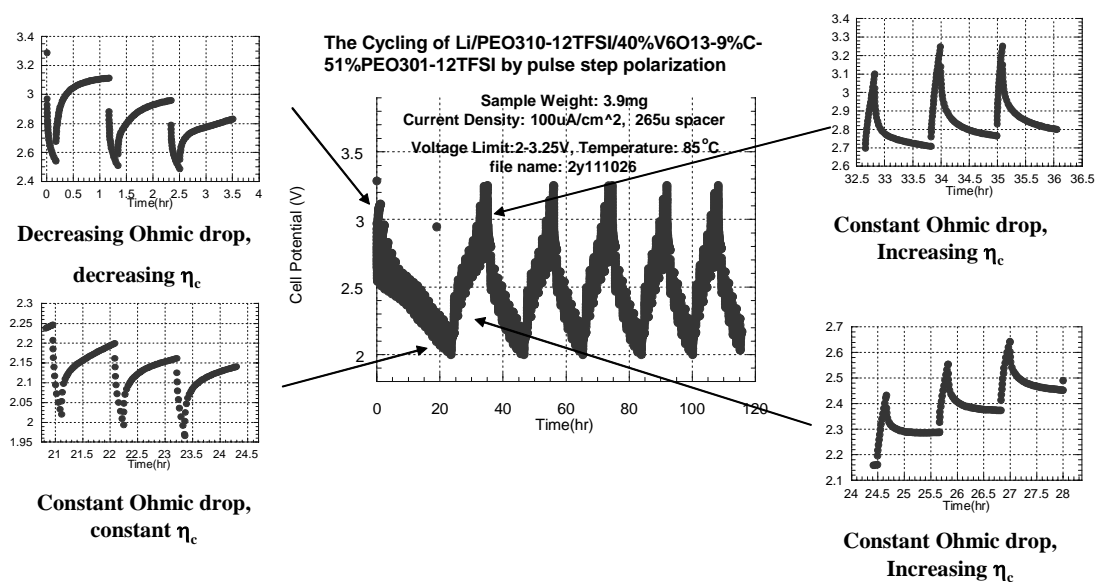


Figure 15. Pulse polarization of a Li metal/PEO-LiTFSI/V<sub>6</sub>O<sub>13</sub> in discharge and charge modes. The cell is charged or discharged for 10 minutes followed by a 1 hour relaxation.

Impedance measurements taken during the course of the cell cycling demonstrates steady increase of impedances (see Figure 16) that are generally identified as the interfacial or charge transfer impedance. Modeling of the impedance response of cells is a complex subject<sup>151</sup>, especially as the response is a mixture of the two electrodes unless steps are taken to introduce a reference electrode. The response can be controlled by solid-state diffusion or electronic conductivity within an electrode, ionic diffusion in the electrolyte phase or interfacial, charge transfer kinetics. In Figure 16 one can observe changes in the impedance as a function of state of charge and the development of several impedances which may be related to processes going on at either or both electrodes. Even more interesting is the observation of dependence of the impedance on the time that the measurement is taken after current is turned off. Figure 17 shows the impedance plots for a lithium/PEO-LiTFSI/lithium cell that is polarized five times in the same direction at 0.2mA/cm<sup>2</sup> for 2 coulombs of charge/cm<sup>2</sup>. The impedance of the cell is taken 30 seconds after the current is turned off (a) and then again after one hour (b). The “charge transfer” impedance is observed to change with time, indicating that some of this impedance is due to salt concentration gradients close to the electrode surface. In some cases the impedance actually decreases with time while in other cases it increases. It can be observed that the impedance appears to return to a similar value indicating that no irreversible process has occurred that would indicate growth of the SEI layer through chemical reactions or the growth of dendrites. In this case, the current density used (0.2mA/cm<sup>2</sup>) was well below the limiting current (>2mA/cm<sup>2</sup>) as calculated from the transport properties and cell geometry. It can further be noted from the time dependence of the impedance spectrum and the increasing polarization observed on passing current that one hour is still not enough time for the concentration gradients to completely relax

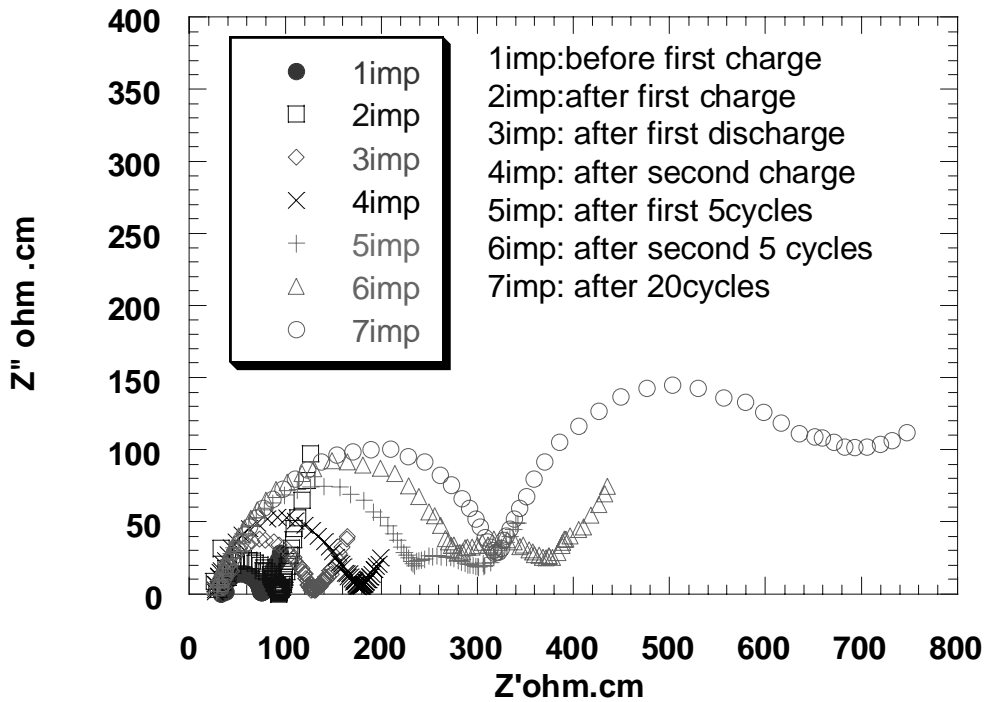


Figure 16. The evolution of impedance in Li/PEO-LiTFSI/V<sub>6</sub>O<sub>13</sub> cells cycled at 100uA/cm<sup>2</sup>

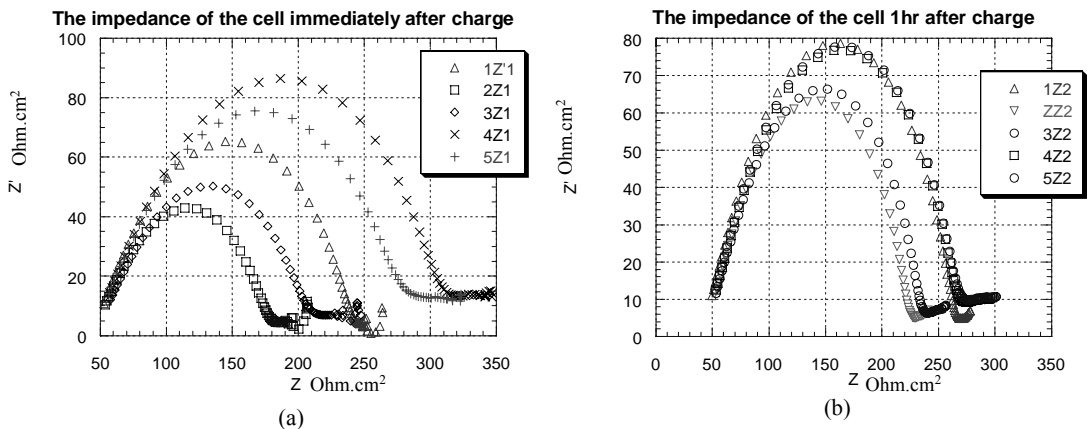


Figure 17. Impedance of a Li/PEO-LiTFSI(1:30)/Li cell at 85°C polarized at 0.2mA/cm<sup>2</sup> for 2 coulombs of charge. Impedance recorded after (a) 30 seconds and (b) one hour after current stopped. Five separate polarizations designated 1-5Z in order.

These observations illustrate that the performance of lithium polymer batteries is dependant upon the behavior of the electrolyte at the interfaces. As noted previously, the



polymer dynamics in composite systems is influenced by the nature of the electrolyte-surface interaction and by the restriction of movement that the presence of the surface causes. Even in the case of the planar lithium metal electrode we have observed significant effects. The salt concentration gradients that build up on the electrodes can lead to depletion on one electrode and very high concentrations that can lead to salt precipitation on the other. Effects of high concentration may also be felt long before actual precipitation occurs. Figure 9 shows that as the salt concentration increases the glass transition temperature of the polymer electrolyte increases. This effect is more severe for EO-containing polymers and is even more pronounced for linear PEO and PPO polymers than the comb polymers shown in Figure 9. The combination of high salt concentration and the interaction with the electrode surface indicates that the electrolyte layer next to the electrode is likely to be very restricted in motion if not actually a glass. This implies that the mechanism of ion transport through these surface layers is different from the bulk and that these layers contribute to the interfacial impedance observed in the polarized cells. Understanding of how ions move such layers is of great importance and the study of ion transport in less mobile polymer systems takes on added relevance in this context<sup>75, 76</sup>.

Figure 9 shows that the dependence of the glass transition temperature upon concentration is much reduced for the TMO-containing polymers and hence they would be expected to generate less interfacial impedance. This is observed at lithium metal electrodes where the TMO comb polymers with LiTFSI typically give an interfacial impedance of about 50 ohm-cm<sup>2</sup> compared to 100 ohm-cm<sup>2</sup> for PEO-LiTFSI. As mentioned above, although the introduction of the TMO groups was disappointing in terms of producing an increase in the bulk conductivity of the polymer electrolytes, the  $t_g$  salt-dependence provides very valuable properties that can lead to greatly improved cell performance by reduction of the interfacial impedance. The importance of interfacial impedance on cell performance can be appreciated by use of system modeling. In the Li/PEMO-LiTFSI/V<sub>6</sub>O<sub>13</sub> model calculations referred to above<sup>124</sup> the interfacial impedances were accounted for by use of a value for the anode film resistance which was taken to be 0.01 ohm-m<sup>2</sup> or 100 ohm-cm<sup>2</sup>. It was found that the peak power that could be obtained from the cell is very dependent on the value that is selected. The results of calculations of peak power that varied this resistance are shown in Figure 18<sup>152</sup>. The decrease in interfacial impedance observed on replacing EO polymers with TMO would lead to a near doubling in the peak power capability. More sobering, however, is the effect of an increase in the interfacial impedance. Since reduction of the cell operating temperature to 25°C typically results in an increase in interfacial impedance to greater than 1 ohm-m<sup>2</sup> even for TMO polymers, this indicates that useful rates of discharge with a polymer electrolyte will not be possible even with high room temperature conductivity unless the interfacial impedance problem is also solved. Thus, the studies of the effects of surfaces on the transport properties take on an even greater importance for all types of batteries and fuel cells.

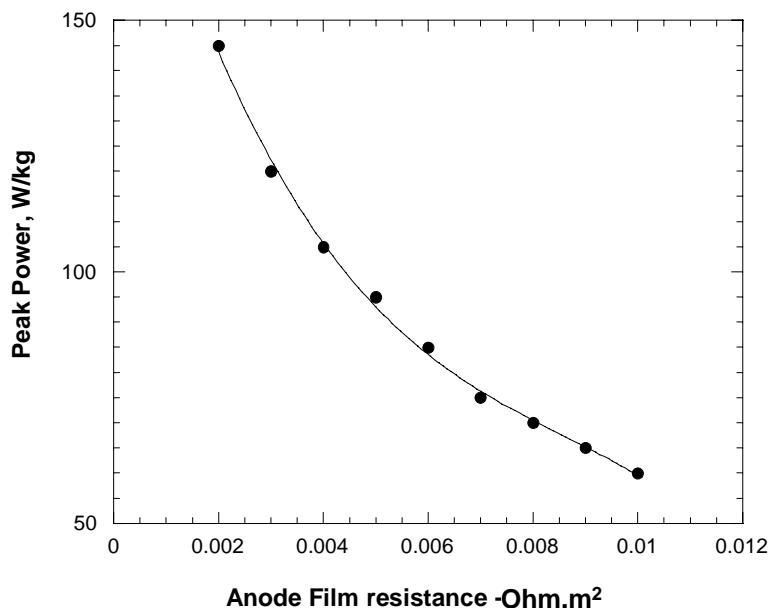


Figure 18 . Dependence of Peak Power on Anode Film (SEI) Resistance<sup>152</sup>.

*Polyelectrolyte Single-Ion Conductors.*

The properties demanded of polymer electrolytes for good performance in lithium batteries that we have discussed now include a forbidding list. In addition to chemical and electrochemical stability, adequate transport properties are necessary both in the bulk of the separator and at the electrode surfaces. This is difficult to attain if the electrochemical processes lead to the development of concentration gradients at the surfaces and the transport properties are degraded at extremes of concentration. A way to avoid this is to use polyelectrolyte single-ion conductor materials which have a transference number  $t_+^0=1$ . With these materials no concentration gradients will develop as the anions are unable to move and accumulate on one side of the cell. However, the loss of anionic mobility results in lower conductivity. The electrolyte portion of the cell is therefore limited by ohmic resistance rather than the concentration polarization. Here again modeling provides invaluable guidance for the design of materials and for targeting appropriate performance goals.

The best known polyelectrolyte material is Nafion<sup>®</sup>, an ionomeric comb polymer with a PTFE backbone and fluorinated ethylene oxide side chains that are terminated with sulfonate anion groups. A number of similar fluorinated materials have been examined for gel polymer systems quite recently<sup>153-155</sup> where the ionomeric membrane is swollen with a solvent. Conductivities greater than  $10^{-4}$ S/cm have been reported. Several attempts have been made to prepare lithium and sodium polyelectrolytes for use in solvent free systems<sup>156-169</sup> and the most successful of these have the comb structure with a

pendant anion similar to the structures shown in Figure 19. A typical comb structure will have several comb side chains with no attached anion for every side chain with an attached anion and this allows the concentration of ions to be controlled<sup>163, 167</sup>. The best conductivities for these polyelectrolytes approach  $10^{-5}$  S/cm at room temperature. The nature of the anion has been shown to play a role through its ability to delocalize the negative charge and hence reduce the strength of ion-pairing to the lithium or sodium ions. Strong ion-pairing as occurs with the alkylsulfonate anion tends to bind the cation and slow its motion through the electrolyte. Replacement of the sulfonate group with fluoroalkylsulfonates leads to a significant increase in conductivity<sup>163</sup>.

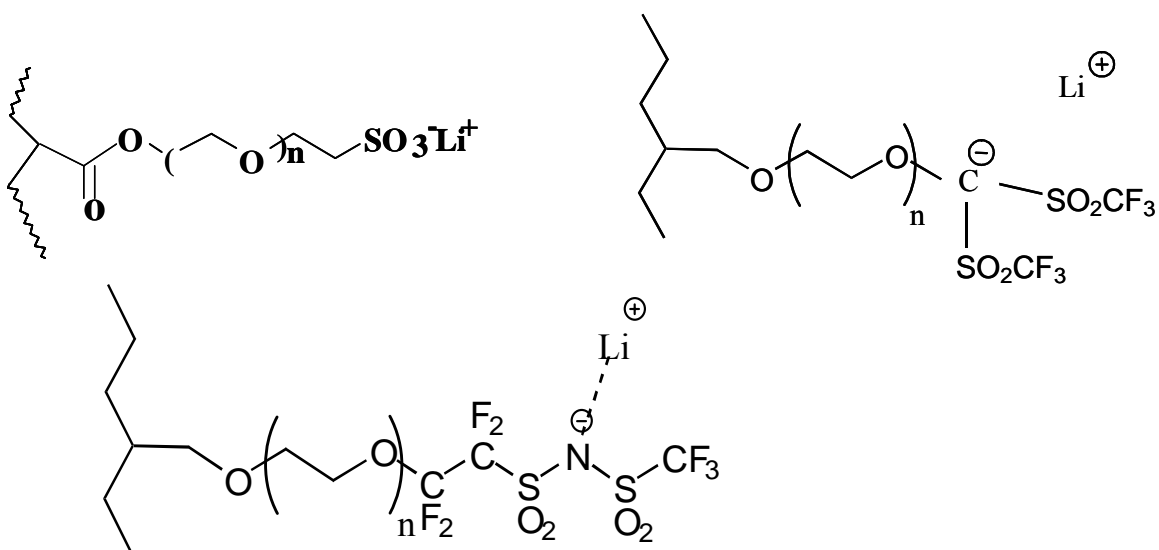


Figure 19. Examples of pendant anions on comb structures for single-ion conductors.

Molecular modeling has been carried out on polyelectrolyte systems using Monte Carlo methods<sup>170, 171</sup>. The results of this modeling imply that the comb-type systems are the optimal architecture when combined with appropriate anions and that the ideal length of the side chains can also be estimated. Comparison with the behavior of the corresponding binary salt systems also allows prediction of the optimum salt concentration for bulk conductivity. It turns out that the optimum ionomer salt concentration is about half that of the binary salt system. This is an important result as the lower salt concentration can lead to lower costs of the electrolyte and probably to better interfacial behavior. A controlling factor in the behavior of the polyelectrolyte is the value of the glass transition temperature. As the ionic concentration increases so does the glass transition temperature and the mobility of the side chains is accordingly diminished. With higher salt concentration there are more charge carriers so that conductivity is increased. Thus an optimum is reached where the ion concentration is maximized before the effect of the rising glass transition temperature reduces the polymer mobility. Here

again, introduction of more flexible backbones and side chains such as the TMO units should depress the  $t_g$  while allowing a higher concentration of ions to be used.

Unfortunately, little work has been reported on the behavior of single-ion conductors in real lithium batteries. Most reports refer only to efforts to increase the conductivities usually because the conductivities are so low as to be impractical. One report exists on the impedance behavior of a polyelectrolyte with sodium electrodes<sup>169</sup> but little satisfactory data has been obtained on the interfacial behavior of polyelectrolytes. System modeling has been employed to estimate the behavior of polyelectrolytes in real cells and to determine the conductivity that is actually needed. The system modeled was the Li/V<sub>6</sub>O<sub>13</sub> cell and the results were compared with the binary salt system using the transport properties shown in Figure 14. For both systems an “ideal” polymer material was modeled and this was the binary salt system at 85°C and a polyelectrolyte system with conductivity of 10<sup>-4</sup>S/cm. An “available” polymer was the binary system at 40°C and a polyelectrolyte with a conductivity of 4 x 10<sup>-6</sup>S/cm which is the conductivity at 40°C of the fluorinated methide anion system shown in Figure 19. The results of the modeling<sup>124</sup> show no clear advantage for either system and both provide rather poor power capability due to the effect of the interfacial resistance. It was also noted that increased power and energy density results from increasing the voltage of the cell which highlights the need to maximize the stability of the electrolyte to high voltage cathodes. The modeling exercise does demonstrate that achievement of lithium polyelectrolyte conductivity between 10<sup>-4</sup> to 10<sup>-3</sup> S/cm at ambient temperatures is a worthwhile goal provided that the interfacial impedance is kept below 50 ohm-cm<sup>2</sup>.

#### Chemical and electrochemical stability of polymer electrolytes.

As we have discussed, the delivery of the lithium ions to the electrode surface is a complicated process. Once there, the dynamics of the layers at the electrode surface is even more difficult to unravel and yet they are critical for the efficiency of the electrochemical reaction. Large surface resistances to electron or ion transfer will lead to slow kinetics, large activation polarizations and side reactions. Side reactions lead to loss of cycling efficiency, capacity fading and an increase of interfacial impedance due to deposition of products at the interface or soluble products that may migrate to other surfaces where reactions may occur that reduce efficiency. Given the inherent reactivity of organic materials to 0V versus Li, it is indeed remarkable that any lithium battery is feasible. The critical role of the SEI layers on the electrodes is the subject of intense investigations<sup>20</sup>. These layers must possess a remarkable set of properties. They must not react with the electrode itself and they must separate the reactive electrode from the sensitive electrolyte. However, the SEI layer must allow the passage of lithium ions with a minimum of resistance. To achieve this degree of selectivity it is necessary that the layers behave as single-ion conductors and that the mechanism of ion conduction is different from the bulk of the solution. The SEI layers must also accommodate changing geometry of the electrode under different states of charge. For intercalation electrodes this involves volume changes as the lithium ion intercalates while for lithium metal shape changes and dendrite growth must be accommodated. In the latter case, changes in the surface area of the electrode occur that expose the electrolyte to fresh lithium metal. The

electrolyte must then participate in the formation of fresh SEI layer to protect against further reaction.

From the previous discussion concerning the effect of surfaces on polymer dynamics, one can appreciate that the passage of the lithium ions through the surface layers is complex indeed. The presence of resistive layers may lead to depletion of ions at the electrode to levels where their concentration can no longer support the current demanded. In such cases electrons must be injected into or removed from other species present in the solution. These species can include the anions of the salt (C-F bond breaking, for example) or the solvent molecules themselves. Detection of fluoride ion demonstrates the reduction of the anion with triflate or TFSI salts. The formation of products from side reactions removes lithium ions from use in the battery and leads to reduced capacity, particularly if the electrode capacities are balanced. Often, however, one electrode is in large excess (e.g. lithium metal) and the loss of lithium is not noticed.

Our understanding of the electrode dynamics may be helped by the chemical side reactions that do occur. The reactive intermediates which lead to irreversible bond cleavage may be related to the mode of electron transfer. It has been shown in the past that electrochemical and chemical reactions may involve different reactive intermediates and these lead to different product distributions<sup>128</sup>. The existence of trapped solvated electrons has been postulated during electrochemically driven electron transfer<sup>172</sup> which will lead to bond cleavage (e.g. carbon-oxygen bonds) once localized on a single solvent molecule. Since a reaction involving an unpaired electron will favor certain structures such as tertiary carbons over secondary or primary carbons, detection of products corresponding to this will support the intermediacy of a radical reactive species. Anionic cleavage will favor secondary over tertiary carbons and this might be expected to occur when two electrons are injected simultaneously as may occur during a chemical reaction between lithium metal surface and solvent molecules. From an analysis of the products formed from suitable solvent molecules (e.g. 2-MeTHF) one can sometimes gain insight into the electrode processes and any corrosion processes that may reduce the capacity of the battery. This understanding can then be used to design electrolytes that are resistant to the side reactions or which have groups deliberately introduced that lead to the formation of desired SEI layers upon reaction.

For linear polymer electrolytes the effect of bond cleavage is to change the molecular weight by breaking the chains and to immobilize the chains on the electrode, possibly leading to poorer ion transport through the surface layer. The detection of changes in molecular weight and mechanical properties are about all that can be gained from linear polymers. Comb polymers are more useful for the investigation of side reactions at electrodes as bond cleavage leads to small fragments that can be detected and quantified by conventional chemical analysis techniques (surface and bulk spectroscopy, gas and liquid chromatography, mass spectroscopy). Figure 20 shows the structure of a comb and how bond cleavage reactions at a negative electrode yield small fragments. Similar reasoning can be applied to oxidation reactions. Different reactive intermediates will favor certain reaction pathways. For example a radical intermediate will favor cleavage of the tertiary carbon in the backbone next to the oxygen while anionic intermediates will favor secondary carbons. Thus electrochemically driven reactions may favor injection of one electron at a time through electron trapping and lead to cleavage at

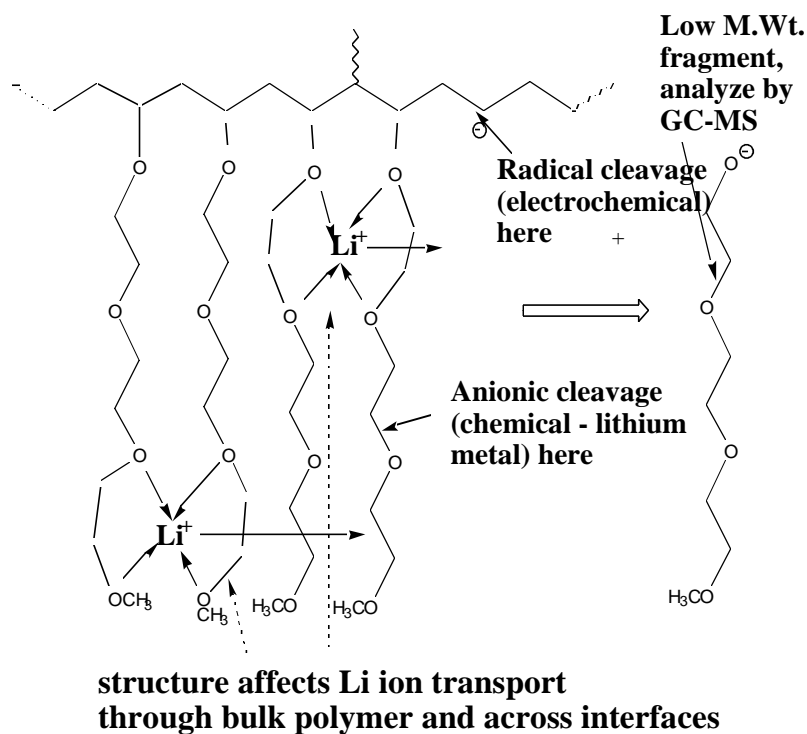


Figure 20. Degradation pathways of polymers at lithium electrodes.

the tertiary carbon and hence the production of fragments that are the full side chain length while corrosion reactions may involve injection of two electrons simultaneously through chemical reaction with the metal surface and yield fragments that result from bond cleavage all along the side chains. The product distribution would then contain products consistent with the preferred point of bond cleavage in the side chain. One may also expect that the cleaved lithium alkoxide fragments will contribute to the SEI layer and influence the behavior of the electrode. The structure of the electrolyte may therefore be designed to provide fragments that promote good interfacial performance and provide a means for SEI layer repair during the battery lifetime. The well known but not understood difference in the interfacial behavior of ethylene carbonate versus propylene carbonate at carbon anodes is an excellent example of this.

The incorporation of functional groups other than ethers in the electrolyte structure has been long studied. Substitution of nitrogen or sulfur for the oxygen<sup>61, 173, 174</sup> not only alters the dielectric constant but also the strength of the donor atom interaction with the lithium ion leading to different solvation energies and different energy barriers to lithium ion movement. As always, however, the reactivity with the electrodes is critical to successful use of a material. The imine and sulfide functions are more easily reduced at the anode than the ether groups and hence the presence of a robust SEI layer is required. As is well known, however, the highly reactive cyclic carbonates are used successfully in lithium ion batteries due to the formation of a remarkable SEI layer<sup>20</sup>. However, other desirable functional groups such as nitrile (e.g. acetonitrile) appear to be unable to form a satisfactory film on lithium metal or on carbon and therefore have very restricted use in lithium batteries.

The ether function reacts with lithium metal also. Figure 21(a) shows some vigorous cycling at 85°C of a symmetrical lithium/lithium cell containing the comb branch polymer PE(TMO)<sub>3</sub> (structure shown in Figure 9) with LiTFSI salt in a 10:1 oxygen:lithium concentration ratio. The cell membrane had a thickness of 256µm and the current density was set at 0.4mA/cm<sup>2</sup>. The cell polarization behavior shows a transition time that indicates the current is operating above the limiting current. The delivery of lithium ions to the electrode is insufficient to support the current and hence a second reaction occurs at a different voltage. One may observe that the cell rapidly fails due to a dendritic short circuit. Extraction of the cell components for analysis by gas chromatography shows the formation of alkoxy alcohols corresponding to cleavage of the side chains as shown in Figure 20 with the (TMO)<sub>3</sub> unit predominating. However, a higher molecular fragment is also seen that corresponds to cleavage of the backbone and indicates more complex behavior than our analysis has so far encompassed.

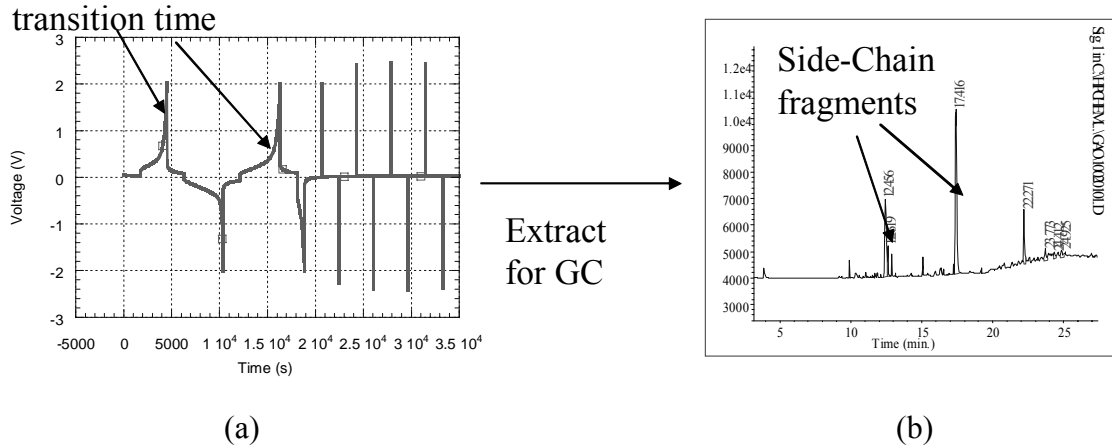


Figure 21.(a) Cycling of Li/PE(TMO)<sub>3</sub>-LiTFSI(10:1)/Li at 85°C and 0.4mA/cm<sup>2</sup>. Cell thickness = 256 µm; (b) Gas chromatogram of extracted membrane from (a).

Prior to the cycling at 0.4mA/cm<sup>2</sup> shown in Figure 21(a) the cell had been cycled at 0.2mA/cm<sup>2</sup> for two days to pass a total of 134 coulombs (37.22mAh) with little visible change in the impedance (< 5% increase in the interfacial impedance). The cell had been cycled during this time at a rate that was below the limiting current where the transport properties were sufficient to ensure an adequate supply of lithium ions. The limiting current  $I_{lim}$  may be calculated according to the following equation<sup>135</sup>:

$$I_{lim} = FD_s \Delta c / (1 - t_+^0) L$$

Where  $F$  = Faraday's constant,  $D_s$  = salt diffusion constant in cm<sup>2</sup>/s,  $\Delta c$  = the concentration difference across the cell in moles/cm<sup>3</sup>,  $t_+^0$  = the lithium ion transference number and  $L$  = the membrane thickness in cm. The salt diffusion coefficient had been measured for this electrolyte using the restricted diffusion method<sup>143</sup>. Estimation of the transference number at about 0.3 allows one to calculate the limiting current and it is

found that  $0.4 \text{ mA/cm}^2$  is above this value, leading to the observation of the transition time shown in Figure 21(a).

While the cell is cycled at values below the limiting current the interfacial impedance does not change appreciably except for concentration effects as shown in Figure 17. This indicates that the SEI layer that is initially formed ( $\text{Li}_2\text{O}$ ,  $\text{LiOH}$ ,  $\text{Li}_2\text{CO}_3$ ,  $\text{LiF}$ ,  $\text{LiOR}$ ) is preventing appreciable reactions between the newly plated lithium and the electrolyte components. However, as soon as the limiting current is reached where insufficient lithium ion is delivered, electrons are injected into the solvent molecules leading to reactions and dendrite growth is initiated. Dendrite growth increases the surface area and reduces the inter-electrode distance therefore increasing the limiting current that may be supported. However, the dendrites frequently grow completely across the gap leading to a short circuit and failure of the cell as shown in Figure 21(a).

### Dendrite Growth.

The role of the transport properties in the initiation and growth of dendrites is well known when the limiting current is exceeded and technological advantage is taken of this to electrodeposit metal powders<sup>175</sup>. If this was the only factor in dendrite growth one could simply ensure that the limiting current was never exceeded and a major problem for lithium metal batteries would be solved. Unfortunately, dendrites also grow at current densities below the calculated limiting current and lead to failure of the cell. Considerable attention has been given to the dendrite problem for both liquid and polymer electrolytes and it remains the most significant issue preventing the commercialization of lithium metal polymer batteries<sup>16, 25, 27, 176-182</sup>. The unpredictable nature of the dendrite growth leads to unacceptable reliability problems as well as safety issues due to the formation of “mossy” lithium deposits. A lot of work has been carried out on liquid electrolyte systems to study lithium dendrite growth but until the last few years the published reports on dendrite growth in polymer electrolytes have been much sparser. Recently a number of excellent *in situ* studies of dendrite growth in PEO electrolytes have appeared<sup>183-193</sup> that demonstrate the growth of dendrites in polymer electrolytes even at current densities that are well below the calculated limiting current. The topic of dendrite growth is covered in detail in a separate chapter in this book so this discussion will be confined to the role of the polymer properties in dendrite growth.

During studies of rechargeable lithium metal anodes in liquid electrolyte systems it was noted that stack pressure on the cells led to improvements in lithium metal cycling<sup>25, 27, 194, 195</sup>. The liquid electrolyte cells contained a microporous separator and through this the pressure was transmitted to the anode surface. These observations led to assumptions that polymer electrolytes would also provide better cycling of the lithium metal electrode. However, the commonly used polymer system, PEO, is a viscous liquid under the typical operation conditions and is not a solid. Some of the recent *in situ* studies have amply demonstrated that dendrites grow rapidly in viscous liquids<sup>183, 186, 188</sup> at current densities well below the limiting current. In experiments carried out in the author’s laboratory, dendrite growth has been observed at virtually any current density provide that the polarization continues for long enough. The rate of initiation and propagation of dendrite growth appears to be sensitive to a number of factors including the presence of impurities<sup>129</sup>, the transport properties and concentration of the salt<sup>38</sup>,



capacity of the charge cycle<sup>68</sup>, the presence of filler particles and the molecular weight which influence the mechanical properties<sup>100</sup>.

For these viscous liquid polymer systems pressure cannot be applied without the aid of a supporting separator network. This can be supplied by use of a microporous separator, addition of nano-particle fillers or by cross-linking the polymer itself. Cross-linking is required<sup>33, 68, 196, 197</sup> to form a true solid electrolyte with the mechanical properties of a solid to inhibit dendrite growth. With an electrolyte with sufficient mechanical strength pressure may be applied to the anode<sup>33, 198</sup> and the dendrite growth further inhibited. Unfortunately, the presence of filler particles and cross-linking tends to raise the glass transition temperature, reduce the mobility of the polymer<sup>33, 68, 100</sup> and the transport properties of the electrolyte decline, leading to a lower limiting current. A further consequence is that any modification of the polymer mechanical properties must be uniform across the membrane. If non-uniform cross-linking or dispersion of particles occurs the current distribution at the anode will be non-uniform and this will encourage dendrite growth. Thus, poorly controlled chemistry such as UV and thermal radical initiated cross-linking is likely to lead to non-uniformity in the polymer membrane and cause problems during cycling particularly at high rates. This is one reason why *in situ* curing of polymer gel systems may not be wise. Development of alternate cross-linking chemistry that is more controllable<sup>35, 197</sup> is critical to the production of quality lithium polymer batteries.

The previous discussion on the effects of surfaces on the polymer dynamics is pertinent to recall at this time. One may recall that the glass transition temperature of polymer electrolytes rises with increasing salt concentration (see figure 9). During discharge of a lithium metal cell with a binary salt system, the concentration gradients at the lithium metal electrode rise to levels that induce phase changes (glass formation, precipitation) and leads to changes in interfacial impedance (figure 17). These changes will be enhanced by the presence of filler particles and cross-links in the polymer and inhomogeneities in the membrane will induce non-uniform current distribution which may encourage dendrite initiation at the opposite electrode in a symmetrical lithium/lithium cell. On charging of the lithium metal electrode in a lithium/polymer/metal oxide cell, the depletion of salt concentration at the plating electrode will lead to a lower  $t_g$ , higher mobility at the electrode surface and the ability to sustain a higher current density. During the charging cycle strong mechanical properties are desired at the plating electrode surface to restrain dendrite growth<sup>33, 68</sup>. However, in the metal oxide electrode, salt concentration rises, leading to a higher  $t_g$ , decreased mobility and high interfacial impedance. The presence of strongly-interacting particles such as carbon black or cross-linking in the polymer electrolyte, binder or polymers formed from electrolyte solvents during the calendar or cycle life will lead to decreased transport properties in the composite electrode. This will be the case for dry polymer, gels and liquid systems and will result in high impedance and low rate capability. The consequence of a non-uniform composite electrode composition will be a very uneven current distribution which will encourage the initiation of dendrite growth at the lithium metal counter electrode.

There is a well-developed literature on morphological instability during electrodeposition of a variety of metals, which indicates that even a small perturbation on the surface will initiate dendrites<sup>199-203</sup>. The case of lithium is complicated by the

reactivity of the metal and the need for a protective film on the surface, commonly known as the SEI. A physical example of a perturbation would be non-uniformity in the SEI that can give rise to instability and dendrite growth. It is obvious from our discussion on polymer dynamics at surfaces how perturbations may arise from the changing properties of the polymer electrolyte during cycling and that any design of polymer electrolytes must take these factors into account. There is much scope for modeling of the effects of such perturbations and how they can induce dendrite growth as cycling is continued. It should be noted that the basis of these models assumes that the surface is fundamentally unstable and that dendrite growth is inevitable. The goal will be to understand how to limit and control the dendrite growth sufficiently for useful battery life.

Mechanical Properties.

The foregoing discussion on dendrite growth highlights the need for better understanding and control of the mechanical properties of the electrolytes. The inevitable desire to push the battery to the limits of its performance will impose great stress on the polymer electrolytes that will rapidly expose any weaknesses. Since the mechanical properties of the polymer electrolytes are closely coupled with the transport properties, the design of the polymer systems needs to take close account of whether it will be used next to a lithium metal electrode, in the bulk of the separator or in a composite electrode. Even the seemingly simple process of cross-linking the polymer membrane can introduce undesirable properties. For example, Figure 22(a) shows the dynamic mechanical thermal analysis (DMTA) of a cross-linked polymer membrane of co-polymer EPE<sub>3</sub> and AGE (10%) with LiTFSI(20:1) that shows the presence of a second  $t_g$  indicating non-uniformity in the material<sup>204</sup>. Examination of the film by contact mode atomic force microscopy (AFM) is shown in Figure 22(b), which shows the presence of non-uniform areas. Phase imaging AFM in tapping mode has been shown to be even more useful for the study of membrane morphology for fuel cell membranes<sup>205</sup> and clearly these are very useful techniques for quality control of membrar

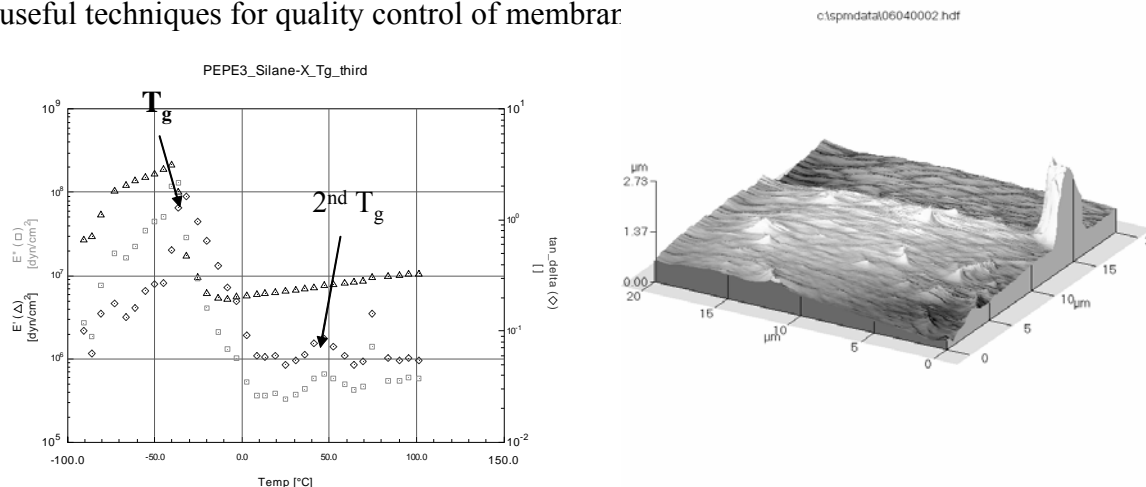


Figure 22. Polymer membranes prepared by cross-linking the co-polymer EPE<sub>3</sub> and AGE (10%) using hydrosilylation<sup>35</sup>; (a) DMTA in compression mode at 10Hz. The elastic ( $E'$ ) and viscous ( $E''$ ) moduli and the  $\tan \delta$  response are shown as a function of temperature. (b) AFM in contact mode.

In this case the non-uniformity of the membrane is due to the non-random nature of the co-polymer. During the co-polymerization it was noted that the AGE and EPE<sub>3</sub> monomers disappeared at different rates indicating that the polymer was a block co-polymer and hence the cross-linking was concentrated in the AGE blocks. The membrane showed rapid formation of dendrites when it was cycled in a symmetrical lithium/lithium cell and this can be ascribed to the non-uniformity of the membrane and the fact that the membrane was very thick (400 $\mu\text{m}$ ) so that the limiting current was low. Unfortunately the requirements for quantitative mechanical measurements ( $\sim 1\text{mm}$  thickness) are difficult to reconcile with the need for thin membranes ( $<50\mu\text{m}$ ) for lithium batteries. Nevertheless, useful results can still be obtained if the membrane can be separated from the electrodes after cycling. Figure 23 shows the frequency sweep (a) and dynamic mechanical thermal analysis (b) of a composite membrane consisting of the cross-linked co-polymer of EPE<sub>3</sub> and AGE (X-PEPE<sub>3</sub>), LiTFSI (20:1) and A200 Aerosil fumed silica before and after cycling at 85 $^{\circ}\text{C}$  in a lithium/lithium cell at 0.2mA/cm<sup>2</sup>. The membrane in this case was about 300 $\mu\text{m}$  thick<sup>204</sup> and the calculated limiting current was about 1mA/cm<sup>2</sup> based on the transport properties measured in the absence of cross-linking and filler particles. The frequency sweep experiments show a decrease in the moduli after cycling while the DMTA shows an increase in the area under the  $\tan \delta$  peak, indicating an increase in the proportion of polymer undergoing the transition, a decrease in the  $t_g$ , indicating increased mobility and the growth of a shoulder on the low temperature side that is a  $\beta$ -transition associated with the movement of the side chains. Extraction of the membrane and analysis by gas chromatography showed the presence of peaks corresponding to cleavage of the side chains and this is consistent with the growth of the  $\beta$ -transition and the loss of mechanical strength from cleavage of the cross-links.

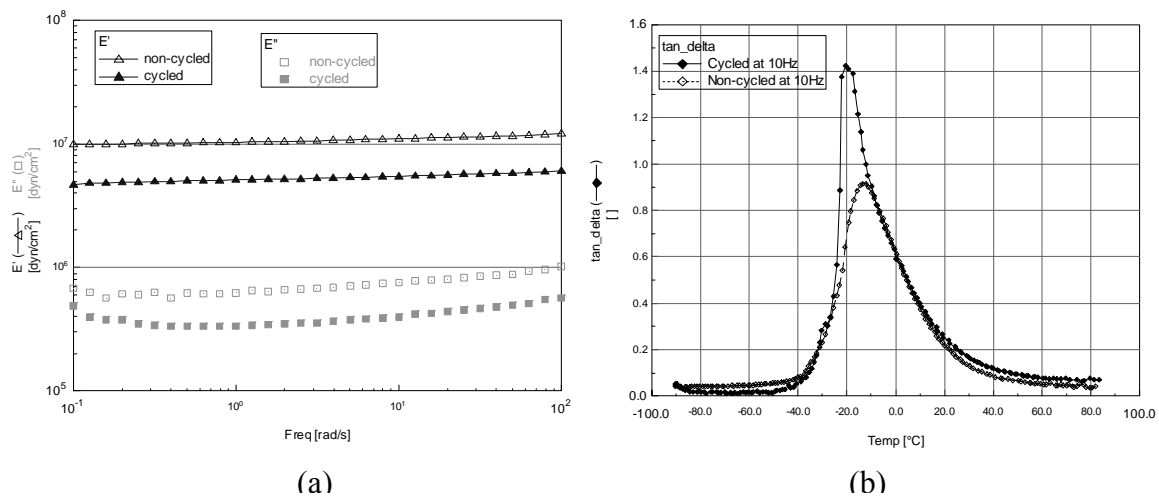


Figure 23. Mechanical measurements on X-linked PEPE<sub>3</sub>-LiTFSI(20:1)-A200 Aerosil (10%) before and after cycling in a Li/Li cell at 85 $^{\circ}\text{C}$ . (a) Frequency sweep; (b) dynamic mechanical thermal analysis at 10Hz<sup>204</sup>.

These results are consistent with the occurrence of bond cleavage during cycling of the lithium metal. Both cross-linking and the presence of strongly interacting filler particles leads to poorer transport and the salt diffusion coefficient was measured to be

reduced by nearly four times by the presence of the cross-linking and the filler particles. Thus, the current density was close to the limiting current and the extent of the damage to the electrolyte may be explained by injection of electrons directly into the polymer under conditions where the supply of lithium ions was insufficient to maintain the current. The loss of mechanical strength observed after cycling shows that chemical reactions at the electrodes can degrade the structure of the membrane during the life of the cell. In this case the degradation appears to be caused by the unexpectedly large decrease in the transport properties due to cross-linking and filler particles which are present to inhibit dendrite growth. This is an apt demonstration of the need to balance transport properties with mechanical properties in lithium batteries as the consequences of chemical reactions with the high energy electrodes is very unforgiving.

## **Conclusions.**

The design of polymer electrolytes for lithium batteries is a complex problem that needs to be approached with a combination of sophisticated modeling, diagnostic techniques and significantly greater synthetic effort than has been applied in the past. Molecular modeling is needed to predict the molecular features desired in an electrolyte to attain the transport properties required to support the desired rate capability and to provide the necessary mechanical strength to act as a separator, inhibit dendrites and to bind together the particles of the composite electrodes. These molecular features must also be stabilized towards reaction at the electrodes by the formation of an SEI layer with almost magical properties. System modeling is needed to set the performance goals of the materials that need to be designed and rigorous comparison of the model predictions with experiment is necessary. Failure analysis must be accomplished by a combination of sophisticated diagnostic techniques together with reaction modeling and synthesis of model materials designed to test the modes of failure. Only then can the rates of side reactions be related to lifetime issues.

It is clear that this task is daunting for dry polymer systems and is likely to prove difficult for polymer gels if demands are put upon them beyond acting as an adhesive to hold lithium ion electrodes together as is mostly practiced today. Our survey of polymer electrolyte properties has demonstrated that the desired properties depend critically upon the component of the cell where the electrolyte has to function. The electrolyte next to lithium metal has to have sufficient mechanical strength to inhibit dendrite growth but the means of attaining this should not reduce the transport properties. The polymer electrolyte in the composite electrodes should have much more flexibility as the surface effects of the electrodes lead to major difficulties with ion transport. This is true in dry polymer, gel and liquid systems where polymers are expected to bind the particles together. These polymer systems also have to resist reactions with these electrodes over the life of the battery so that these desirable properties do not change and degrade the performance of the battery.

Given all of these rigorous requirements, it is hardly surprising that the introduction of the lithium metal polymer battery has not yet been successful. In fact, it is more surprising that progress has been as successful as it has been given how primitive have been the polymer systems used so far in comparison to the severity of the demands placed on them by battery engineers. This chapter has attempted to illustrate how

modeling, diagnostics and synthesis can be used to design better materials for the application. Many of these methods have only become available in recent years so there is much exciting work to be done in the coming years. The lithium metal system is particularly difficult due to the dendrite issue but holds the most promise for a very high energy density, particularly if ways can be found to increase the cell voltage to 4 volts or more. This will require the development of multi-layer systems that have a layer resistant to lithium metal on the lithium with high mechanical strength and a polymer in the cathode that is stable to four volts. Since no single material can combine these chemical properties different materials will be necessary in different parts of the cell. As we have seen, it is necessary for the electrolyte to possess different mechanical properties in different parts of the cell anyway. The nature of these multilayers next to electrodes will be the subject of much research and it is encouraging to note that already attempts are being made to design and fabricate protective layers on both anodes and cathodes<sup>206-208</sup>. Such efforts are likely only the beginning of an exciting new chapter in the development of lithium batteries which will lead to more realistic demands on the battery materials and better designed materials for the applications.

### **Acknowledgement.**

This work was supported by the Assistant Secretary for Energy Efficiency and Renewable Energy, Office of FreedomCAR and Vehicle Technologies of the U.S. Department of Energy under Contract No. DE-AC03-76SF00098.

### **References**

1. R. T. Leah, N. P. Brandon, V. Vesovic, and G. H. Kelsall, *Journal of the Electrochemical Society* **147** 4173 2000.
2. J. A. Kerres, *Journal of Membrane Science* **185** 3 2001.
3. K. D. Kreuer, *Journal of Membrane Science* **185** 29 2001.
4. S. Mazrou, H. Kerdjoudj, A. T. Cherif, A. Elmidaoui, and J. Molenat, *New Journal of Chemistry* **22** 355 1998.
5. L. Bazinet, F. Lamarche, and D. Ippersiel, *Trends in Food Science & Technology* **9** 107 1998.
6. D. E. Fenton, J. M. Parker, and P. V. Wright, *Polymer* **14** 589 1973.
7. P. V. Wright, *Br. Polymer J.* **7** 319 1975.
8. M. Armand, J. Y. Sanchez, M. Gauthier, and Y. Choquette, in *Electrochemistry of Novel Materials* (J. Lipkowski and P. N. Ross, eds.), VCH, New York, NY, 1994, p. 65.
9. M. Armand, *Solid State Ionics* **69** 309 1994.
10. M. A. Ratner, (J. R. MacCallum and C. A. Vincent, eds.), Elsevier Applied Science, London ; New York, 1987, p. x.
11. J. R. MacCallum and C. A. Vincent, *Polymer electrolyte reviews--2*, Elsevier Applied Science, London ; New York, 1989.
12. F. M. Gray, *Solid polymer electrolytes : fundamentals and technological applications*, VCH, New York, NY, 1991.
13. F. M. Gray and Royal Society of Chemistry (Great Britain), *Polymer electrolytes*, Royal Society of Chemistry, Cambridge, 1997.
14. P. V. Wright, *MRS Bulletin* **27** 597 2002.
15. B. Scrosati and C. A. Vincent, *MRS Bulletin* **25** 28 2000.
16. D. Fauteux, A. Massucco, M. McLin, M. Vanburen, and J. Shi, *Electrochimica Acta* **40** 2185 1995.
17. M. A. Ratner, P. Johansson, and D. F. Shriver, *Mrs Bulletin* **25** 31 2000.
18. M. A. Ratner and D. F. Shriver, *MRS Bulletin* **39** 1989.
19. A. Hooper, M. Gauthier, and A. Belanger, *Electrochem. Sci. Technol. Polym.* **2** 375 1990.

20. D. Aurbach, in *Advances in lithium-ion batteries* (W. A. v. Schalkwijk and B. Scrosati, eds.), Kluwer Academic/Plenum Publishers, New York, NY, 2002, p. 7.
21. S. E. Sloop, J. K. Pugh, S. Wang, J. B. Kerr, and K. Kinoshita, *Electrochemical & Solid-State Letters* **4** A42 2001.
22. L. Vogdanis, B. Martens, H. Uchtmann, F. Hensel, and W. Heitz, *Makromol. Chem.* **191** 465 1990.
23. J. L. Goldman, L. A. Dominey, and V. R. Koch, *Journal of Power Sources* **26** 519 1989.
24. Y. Gofer, M. Benzion, and D. Aurbach, *Journal of Power Sources* **39** 163 1992.
25. K. M. Abraham, *Electrochimica Acta* **38** 1233 1993.
26. V. R. Koch, *J. Electrochemical Society* **128** 1293 1981.
27. K. M. Abraham, J. S. Foos, and J. L. Goldman, *J. Electrochemical Society* **131** 2197 1984.
28. S.-J. Wen, J. Kerr, M. Rubin, J. Slack, and K. von Rottkay, *Solar Energy Materials & Solar Cells*. **56** 299 1999.
29. G. Oradd, L. Edman, and A. Ferry, *Solid State Ionics* **152** 131 2002.
30. Y. G. Andreev and P. G. Bruce, *Electrochimica Acta* **45** 1417 2000.
31. Y. G. Andreev and P. G. Bruce, *Journal of Physics-Condensed Matter* **13** 8245 2001.
32. D. J. Wilson, C. V. Nicholas, R. H. Mobbs, and C. Booth, *British Polymer Journal* **22** 129 1990.
33. A. Vallee, M. Duval, F. Brochu, M. Kono, E. Hayashi, and T. Sada, *USP* 5,755,985, 1998
34. H. R. Allcock, *Chemistry of Materials* **6** 1476 1994.
35. H. R. Allcock, D. E. Smith, Y. B. Kim, and J. J. Fitzgerald, *Macromolecules* **27** 5206 1994.
36. J. M. G. Cowie, V. M. C. Reid, and I. J. McEwen, *British Polymer Journal* **23** 353 1990.
37. J. M. G. Cowie and A. C. S. Martin, *Polymer* **32** 2411 1991.
38. O. Buriez, Y. B. Han, J. Hou, J. B. Kerr, J. Qiao, S. E. Sloop, M. M. Tian, and S. G. Wang, *Journal of Power Sources* **89** 149 2000.
39. S. Pantaloni, S. Passerini, F. Croce, B. Scrosati, F. Roggero, and M. Andrei, *Electrochimica Acta* **34** 635 1989.
40. L. Marchese, M. Andrei, A. Roggero, S. Passerini, P. Prospero, and B. Scrosati, *Electrochimica Acta* **37** 1559 1992.
41. M. Andrei, L. Marchese, S. Passerini, A. Roggero, and B. Scrosati, *USA*, 5,162,174, 1992
42. M. Andrei, L. Marchese, P. Prospero, and A. Roggero, *USA* 5,173,205, 1992
43. M. Andrei, L. Marchese, A. Roggero, and P. Prospero, *Solid State Ionics* **72** 140 1994.
44. J. M. G. Cowie and K. Sadaghianizadeh, *Solid State Ionics* **42** 243 1990.
45. P. M. Blonsky, D. F. Shriver, P. Austin, and H. R. Allcock, *Journal Of the American Chemical Society* **106** 6854 1984.
46. H. R. Allcock, S. J. M. Oconnor, D. L. Olmeijer, M. E. Napierala, and C. G. Cameron, *Macromolecules* **29** 7544 1996.
47. H. R. Allcock, D. L. Olmeijer, and S. J. M. Oconnor, *Macromolecules* **31** 753 1998.
48. Z. C. Zhang and S. B. Fang, *Electrochimica Acta* **45** 2131 2000.
49. R. Hooper, L. J. Lyons, D. A. Moline, and R. West, *Organometallics* **18** 3249 1999.
50. A. Nishimoto, M. Watanabe, Y. Ikeda, and S. Kohjiya, *Electrochimica Acta* **43** 1177 1998.
51. M. Kono, E. Hayashi, and M. Watanabe, *Journal of the Electrochemical Society* **145** 1521 1998.
52. M. Watanabe, T. Endo, A. Nishimoto, K. Miura, and M. Yanagida, *Journal of Power Sources* **82** 786 1999.
53. A. Nishimoto, K. Agehara, N. Furuya, T. Watanabe, and M. Watanabe, *Macromolecules* **32** 1541 1999.
54. G. M. Mao, R. F. Perea, W. S. Howells, D. L. Price, and M. L. Saboungi, *Nature* **405** 163 2000.
55. G. M. Mao, M. L. Saboungi, D. L. Price, M. B. Armand, and W. S. Howells, *Physical Review Letters* **84** 5536 2000.
56. M. L. Saboungi, D. L. Price, G. M. Mao, R. Fernandez-Perea, O. Borodin, G. D. Smith, M. Armand, and W. S. Howells, *Solid State Ionics* **147** 225 2002.
57. J. W. Halley and Y. H. Duan, *Journal of Power Sources* **89** 139 2000.
58. O. Borodin, G. D. Smith, and R. L. Jaffe, *Journal of Computational Chemistry* **22** 641 2001.
59. A. Aabloo, M. Klintonberg, and J. O. Thomas, *Electrochimica Acta* **45** 1425 2000.
60. H. Kasemagi, M. Klintonberg, A. Aabloo, and J. O. Thomas, *Solid State Ionics* **147** 367 2002.
61. P. Johansson, *Polymer* **42** 4367 2001.
62. G. J. Kearley, P. Johansson, R. G. Delaplane, and J. Lindgren, *Solid State Ionics* **147** 237 2002.
63. P. C. Redfern and L. A. Curtiss, *Journal of Power Sources* **110** 401 2002.

64. J. M. G. Cowie, (J. R. MacCallum and C. A. Vincent, eds.), Elsevier Applied Science, London ; New York, 1987, p. x.
65. A. Sutjianto and L. A. Curtiss, *Journal of Physical Chemistry* 102 968 1998.
66. A. G. Baboul, P. C. Redfern, A. Sutjianto, and L. A. Curtiss, *Journal of the American Chemical Society* 121 7220 1999.
67. J. B. Kerr, G. Liu, L. A. Curtiss, and P. C. Redfern, *Electrochimica Acta* In press 2003.
68. J. B. Kerr, S. E. Sloop, G. Liu, Y. B. Han, J. Hou, and S. Wang, *Journal of Power Sources* 110 389 2002.
69. A. V. G. Ruzette, P. P. Soo, D. R. Sadoway, and A. M. Mayes, *Journal of the Electrochemical Society* 148 A537 2001.
70. P. P. Soo, B. Y. Huang, Y. I. Jang, Y. M. Chiang, D. R. Sadoway, and A. M. Mayes, *Journal of the Electrochemical Society* 146 32 1999.
71. P. E. Trapa, B. Y. Huang, Y. Y. Won, D. R. Sadoway, and A. M. Mayes, *Electrochemical & Solid-State Letters* 5 A85 2002.
72. Y. Zheng, F. Chia, G. Ungar, and P. V. Wright, *Journal of Power Sources* 97-8 641 2001.
73. Y. G. Zheng, F. S. Chia, G. Ungar, T. H. Richardson, and P. V. Wright, *Electrochimica Acta* 46 1397 2001.
74. F. S. Chia, Y. Zheng, J. Liu, G. Ungar, and P. V. Wright, *Solid State Ionics* 147 275 2002.
75. X. Y. Wei and D. F. Shriver, *Chemistry of Materials* 10 2307 ff. 1998.
76. Z. Gadjourova, Y. G. Andreev, D. P. Tunstall, and P. G. Bruce, *Nature* 412 520 2001.
77. M. G. McLin and C. A. Angell, *Solid State Ionics* 53-56 1027 1992.
78. F. Croce, G. B. Appetecchi, L. Persi, and B. Scrosati, *Nature* V394 456 1998.
79. L. Persi, F. Croce, B. Scrosati, E. Plichta, and M. A. Hendrickson, *Journal of the Electrochemical Society* V149 A212 2002.
80. D. Golodnitsky, G. Ardel, E. Strauss, E. Peled, Y. Lareah, and Y. Rosenberg, *Journal of the Electrochemical Society* V144 3484 1997.
81. D. Golodnitsky, G. Ardel, and E. Peled, *Solid State Ionics* V147 141 2002.
82. B. Kumar and L. G. Scanlon, *Journal of Electroceramics* V5 127 2000.
83. B. Kumar, L. G. Scanlon, and R. J. Spry, *Journal of Power Sources* 96 337 2001.
84. P. Johansson, M. A. Ratner, and D. F. Shriver, *Journal of Physical Chemistry B* 105 9016 2001.
85. J. E. Weston and B. C. H. Steele, *Solid State Ionics* 7 81 1982.
86. J. E. Weston and B. C. H. Steele, *Solid State Ionics* 7 1982.
87. G. Tsagaropoulos and A. Eisenberg, *Macromolecules* 28 396 1995.
88. G. Tsagaropoulos and A. Eisenberg, *Macromolecules* 28 6067 1995.
89. S. Gagliardi, V. Arrighi, R. Ferguson, and M. T. F. Telling, *Physica B* 301 110 2001.
90. A. Zhu and S. S. Sternstein, in *MRS*, Vol. 661 (A. I. Nakatani, R. P. Hjelm, M. Gerspacher, and R. Krishnamoorti, eds.), MRS, Boston, MA, 2000, p. KK4.3.1.
91. W. E. Wallace, D. A. Fischer, K. Efimenko, W. L. Wu, and J. Genzer, *Macromolecules* 34 5081 2001.
92. W. E. Wallace, J. H. Vanzanten, and W. L. Wu, *Physical Review A* 52 R3329 1995.
93. J. H. Vanzanten, W. E. Wallace, and W. L. Wu, *Physical Review A* 53 R2053 1996.
94. J. A. Forrest and J. Mattsson, *Physical Review E* 61 R53 2000.
95. J. A. Forrest, J. Mattsson, and L. Borjesson, *European Physical Journal A* 8 129 2002.
96. J. A. Forrest, K. Dalnoki-Veress, J. R. Stevens, and J. R. Dutcher, *Physical Review Letters* 77 2002 1996.
97. J. A. Forrest and K. Dalnoki-Veress, *Advances in Colloid & Interface Science* 94 167 2001.
98. V. L. Vakula and L. M. Pritykin, *Polymer adhesion : physico-chemical principles*, E. Horwood, London, 1991.
99. S. H. Anastasiadis, A. Karim, and G. S. Ferguson, *Interfaces, adhesion and processing in polymer systems : symposium held April 24-27, 2000, San Francisco, California, U.S.A.*, Materials Research Society, Warrendale, Penn., 2001.
100. J. B. Kerr, J. Xie, and R. Duan, *Journal of the Electrochemical Society* Submitted 2003.
101. D. R. Sadoway, B. Y. Huang, P. E. Trapa, P. P. Soo, P. Bannerjee, and A. M. Mayes, *Journal of Power Sources* 97-8 621 2001.
102. H. Lund and O. Hammerich, *Organic electrochemistry : an introduction and a guide*, Marcel Dekker, New York, 2001.
103. O. Hammerich and V. D. Parker, *Electrochimica Acta* 18 537 1973.

104. G. B. Appetecchi, F. Croce, L. Persi, F. Ronci, and B. Scrosati, *Electrochimica Acta* V45 1481 2000.
105. Y. Nishi, in *Advances in lithium-ion batteries* (W. A. v. Schalkwijk and B. Scrosati, eds.), Kluwer Academic/Plenum Publishers, New York, NY, 2002, p. 233.
106. B. Scrosati, in *Advances in lithium-ion batteries* (W. A. v. Schalkwijk and B. Scrosati, eds.), Kluwer Academic/Plenum Publishers, New York, NY, 2002, p. 251.
107. M. Kono, E. Hayashi, and M. Watanabe, *Journal of the Electrochemical Society* 146 1626 1999.
108. M. Kono, E. Hayashi, M. Nishiura, and M. Watanabe, *Journal of the Electrochemical Society* 147 2517 2000.
109. A. S. Gozdz, C. N. Scmutz, and J.-M. Tarascon, US, 1994
110. M. Doyle, J. Newman, A. S. Gozdz, C. N. Scmutz, and J. M. Tarascon, *Journal of the Electrochemical Society* 143 1890 1996.
111. P. Arora, M. Doyle, A. S. Gozdz, R. E. White, and J. Newman, *Journal of Power Sources* 88 219 2000.
112. A. Du Pasquier, P. C. Warren, D. Culver, A. S. Gozdz, G. G. Amatucci, and J. M. Tarascon, *Solid State Ionics* 135 249 2000.
113. A. Du Pasquier, T. Zheng, G. G. Amatucci, and A. S. Gozdz, *Journal of Power Sources* 97-8 758 2001.
114. Y. Aihara, G. B. Appetecchi, B. Scrosati, and K. Hayamizu, *Physical Chemistry Chemical Physics* 4 3443 2002.
115. Y. Aihara, G. B. Appetecchi, and B. Scrosati, *Journal of the Electrochemical Society* 149 A849 2002.
116. J. M. Tarascon, A. S. Gozdz, C. Scmutz, F. Shokoohi, and P. C. Warren, *Solid State Ionics* 86-8 49 1996.
117. S. A. Khan, G. L. Baker, and S. Colson, *Chemistry of Materials* V6 2359 1994.
118. J. Fan, S. R. Raghavan, X. Y. Yu, S. A. Khan, P. S. Fedkiw, J. Hou, and G. L. Baker, *Solid State Ionics* V111 117 1998.
119. S. R. Raghavan, M. W. Riley, P. S. Fedkiw, and S. A. Khan, *Chemistry of Materials* V10 244 1998.
120. H. J. Walls, J. Zhou, J. A. Yerian, P. S. Fedkiw, S. A. Khan, M. K. Stowe, and G. L. Baker, *Journal of Power Sources* V89 156 2000.
121. H. L. Dai and T. A. Zawodzinski, *Journal of the Electrochemical Society* 143 L 107 1996.
122. H. L. Dai and T. A. Zawodzinski, *Journal of Electroanalytical Chemistry* 459 111 1998.
123. A. Eisenberg and J.-S. Kim, *Introduction to Ionomers*, Wiley, New York, NY, 1998.
124. K. E. Thomas, S. E. Sloop, J. B. Kerr, and J. Newman, *Journal of Power Sources* 89 132 2000.
125. K. E. Thomas, R. M. Darling, and J. Newman, in *Advances in lithium-ion batteries* (W. A. v. Schalkwijk and B. Scrosati, eds.), Kluwer Academic/Plenum Publishers, New York, NY, 2002, p. 345.
126. D. R. Sadoway and A. M. Mayes, *MRS Bulletin* 27 590 2002.
127. P. N. Powell, *Laser Focus World* 37 41 2001.
128. J. B. Kerr, *Journal of the Electrochemical Society* 132 2839 1985.
129. O. Chusid, Y. Gofer, D. Aurbach, M. Watanabe, T. Momma, and T. Osaka, *Journal of Power Sources* 97-8 632 2001.
130. W. Schmidt and E. Steckhan, *Angew. Chem.* 91 850 1979.
131. W. Schmidt and E. Steckhan, *Angew. Chem.* 90 717 1978.
132. J. W. Boyd, P. Schmazzl, and L. L. Miller, *Journal of the American Chemical Society* 102 3856 1980.
133. X. R. Zhang, J. K. Pugh, and P. N. Ross, *Journal of the Electrochemical Society* 148 E183 2001.
134. M. Moshkovich, M. Cojocar, H. E. Gottlieb, and D. Aurbach, *Journal of Electroanalytical Chemistry* 497 84 2001.
135. J. Newman, *Electrochemical Systems*, Prentice-Hall, Englewood Cliffs, NJ, 1991.
136. M. Doyle and J. Newman, *Journal of Power Sources* 54 46 1995.
137. M. Doyle and J. Newman, *Electrochimica Acta* 40 2191 1995.
138. M. Doyle, T. F. Fuller, and J. Newman, *Electrochimica Acta* 39 2073 1994.
139. T. F. Fuller, M. Doyle, and J. Newman, *Journal of the Electrochemical Society* 141 1 1994.
140. T. F. Fuller, M. Doyle, and J. Newman, *Journal of the Electrochemical Society* 141 982 1994.
141. M. Doyle, T. F. Fuller, and J. Newman, *Journal of the Electrochemical Society* 140 1526 1993.
142. A. Ferry, M. M. Doeff, and L. C. Dejonghe, *Electrochimica Acta* 43 1387 1998.
143. Y. P. Ma, M. Doyle, T. F. Fuller, M. M. Doeff, L. C. Dejonghe, and J. Newman, *Journal of the Electrochemical Society* 142 1859 1995.



144. H. J. Walls and T. A. Zawodzinski, *Electrochemical & Solid-State Letters* 3 321 2000.
145. A. Ferry, M. M. Doeff, and L. C. Dejonghe, *Journal of the Electrochemical Society* 145 1586 1998.
146. M. M. Doeff, P. Georen, J. Qiao, J. Kerr, and L. C. De Jonghe, *Journal of the Electrochemical Society* 146 2024 1999.
147. M. M. Doeff, L. Edman, S. E. Sloop, J. Kerr, and L. C. De Jonghe, *Journal of Power Sources* 89 227 2000.
148. L. Edman, M. M. Doeff, A. Ferry, J. Kerr, and L. C. De Jonghe, *Journal of Physical Chemistry B* 104 3476 2000.
149. M. M. Doeff, A. Ferry, Y. P. Ma, L. Ding, and L. C. Dejonghe, *Journal of the Electrochemical Society* 144 L 20 1997.
150. L. F. Nazar, G. Goward, F. Leroux, M. Duncan, H. Huang, T. Kerr, and J. Gaubicher, *International Journal of Inorganic Materials* 3 191 2001.
151. M. Doyle, J. P. Meyers, and J. Newman, *Journal of the Electrochemical Society* 147 99 2000.
152. E. Rivero, K. O. Thomas, and J. Newman, Unpublished results 2002.
153. M. Doyle, M. E. Lewittes, M. G. Roelofs, and S. A. Perusich, *Journal of Physical Chemistry B* 105 9387 2001.
154. M. Doyle, M. E. Lewittes, M. G. Roelofs, S. A. Perusich, and R. E. Lowrey, *Journal of Membrane Science* 184 257 2001.
155. A. E. Feiring, S. K. Choi, M. Doyle, and E. R. Wonchoba, *Macromolecules* 33 9262 2000.
156. D. P. Siska and D. F. Shriver, *Chemistry of Materials* 13 4698 2001.
157. T. Fujinami, A. Tokimune, M. A. Mehta, D. F. Shriver, and G. C. Rawsy, *Chemistry of Materials* 9 2236 1997.
158. K. Matsushita, Y. Shimazaki, M. A. Mehta, and T. Fujinami, *Solid State Ionics* 133 295 2000.
159. M. A. Mehta and T. Fujinami, *Chemistry Letters* 915 1997.
160. G. C. Rawsy, T. Fujinami, and D. F. Shriver, *Chemistry of Materials* 6 2208 1994.
161. D. Benrabah, M. Armand, and D. Delabouglise, *USP* 5,696,224, 1997
162. D. Benrabah, S. Sylla, F. Alloin, and M. Armand, *Electrochimica Acta* 40 2259 1995.
163. J. M. G. Cowie and G. H. Spence, *Solid State Ionics* 123 233 1999.
164. D. D. Desmarteau, *Journal of Fluorine Chemistry* 72 203 1995.
165. L. Q. Hu and D. D. Desmarteau, *Inorganic Chemistry* 32 5007 1993.
166. W. Xu, K. S. Siow, Z. Gao, and S. Y. Lee, *Chem. Mater.* 10 1951 1998.
167. S. S. Zhang and G. X. Wan, *Journal of Applied Polymer Science* 48 405 1993.
168. S. S. Zhang, L. L. Yang, and Q. G. Liu, *Solid State Ionics* 76 121 1995.
169. S. S. Zhang, L. L. Yang, and Q. G. Liu, *Solid State Ionics* 76 127 1995.
170. J. F. Snyder, M. A. Ratner, and D. F. Shriver, *Solid State Ionics* 147 249 2002.
171. J. F. Snyder, M. A. Ratner, and D. F. Shriver, *Journal of the Electrochemical Society* 148 A858 2001.
172. D. Rahner, *Journal of Power Sources* 82 358 1999.
173. R. E. A. Dillon and D. F. Shriver, *Chemistry of Materials* 13 1369 2001.
174. S. York, R. Frech, A. Snow, and D. Glatzhofer, *Electrochimica Acta* 46 1533 2001.
175. M. Paunovic, M. Schlesinger, and Electrochemical Society, *Fundamentals of electrochemical deposition*, Wiley, New York, 1998.
176. D. Aurbach, E. Zinigrad, H. Teller, and P. Dan, *Journal of the Electrochemical Society* 147 1274 2000.
177. J. O. Besenhard, J. Guertler, P. Komenda, and M. Josowicz, *Proc. - Electrochem. Soc.* 88-6 618 1988.
178. D. Fauteux, *Electrochimica Acta* 38 1199 1993.
179. D. Fauteux and R. Koksang, *Journal Of Applied Electrochemistry* 23 1 1993.
180. K. Kanamura, *Erekutoronikusu* 43 60 1998.
181. Z.-i. Takehara, *J. Power Sources* 68 82 1997.
182. J.-i. Yamaki, S.-i. Tobishima, K. Hayashi, K. Saito, Y. Nemoto, and M. Arakawa, *J. Power Sources* 74 219 1998.
183. M. Rosso, T. Gobron, C. Brissot, J. N. Chazalviel, and S. Lascaud, *Journal of Power Sources* 97-8 804 2001.
184. C. Brissot, M. Rosso, J. N. Chazalviel, and S. Lascaud, *Journal of Power Sources* 94 212 2001.
185. C. Brissot, M. Rosso, J. N. Chazalviel, and S. Lascaud, *Journal of the Electrochemical Society* 146 4393 1999.
186. C. Brissot, M. Rosso, J. N. Chazalviel, and S. Lascaud, *Journal of Power Sources* 82 925 1999.

187. C. Brissot, M. Rosso, J. N. Chazalviel, P. Baudry, and S. Lascaud, *Electrochimica Acta* 43 1569 1998.
188. M. Dolle, L. Sannier, B. Beaudoin, M. Trentin, and J. M. Tarascon, *Electrochemical & Solid-State Letters* 5 A286 2002.
189. F. Orsini, L. Dupont, B. Beaudoin, S. Grugeon, and J. M. Tarascon, *International Journal of Inorganic Materials* 2 701 2000.
190. F. Orsini, M. Dolle, and J. M. Tarascon, *Solid State Ionics* 135 213 2000.
191. F. Orsini, A. du Pasquier, B. Beaudouin, J. M. Tarascon, M. Trentin, N. Langenhuizen, E. de Beer, and P. Notten, *Journal of Power Sources* 82 918 1999.
192. F. Orsini, A. Dupasquier, B. Beaudoin, J. M. Tarascon, M. Trentin, N. Langenhuizen, E. Debeer, and P. Notten, *Journal of Power Sources* 76 19 1998.
193. T. Osaka, T. Homma, T. Momma, and H. Yarimizu, *J. Electroanal. Chem.* 421 153 1997.
194. J. A. R. Stiles, K. Brandt, D. S. Wainwright, and K. C. Lee, USP 4,587,182, 1986
195. E. Eweka, J. R. Owen, and A. Ritchie, *Journal of Power Sources* 65 247 1997.
196. T. Tatsuma, M. Taguchi, and N. Oyama, *Electrochimica Acta* 46 1201 2001.
197. C. Michot, A. Vallee, P.-E. Harvey, M. Gauthier, and M. Armand, USP 6,492,449, 2002
198. M. Gauthier, A. Belanger, and A. Vallee, USP 6,007,935, 1999
199. J. Elezgaray, C. Leger, and F. Argoul, *Journal of the Electrochemical Society* 145 2016 1998.
200. D. S. Louch and M. D. Pritzker, *Journal of Electroanalytical Chemistry and Interfacial Electrochemistry* 319 33 1991.
201. D. S. Louch and M. D. Pritzker, *Journal of Electroanalytical Chemistry* 346 211 1993.
202. L. G. Sundstrom and F. H. Bark, *Electrochimica Acta* 40 599 1995.
203. M. D. Pritzker and T. Z. Fahidy, *Electrochimica Acta* 37 103 1992.
204. J. Xie, G. Liu, Y. B. Han, and K. J.B., Unpublished results 2003.
205. F. Wang, M. Hickner, Y. S. Kim, T. A. Zawodzinski, and J. E. McGrath, *Journal of Membrane Science* 197 231 2002.
206. S. J. Visco and F. Y. Tsang, USP 6,432,584, 2002
207. S. J. Visco and M.-Y. Chu, USP 6,025,094, 2000
208. N. J. Dudney, *Journal of Power Sources* 89 176 2000.